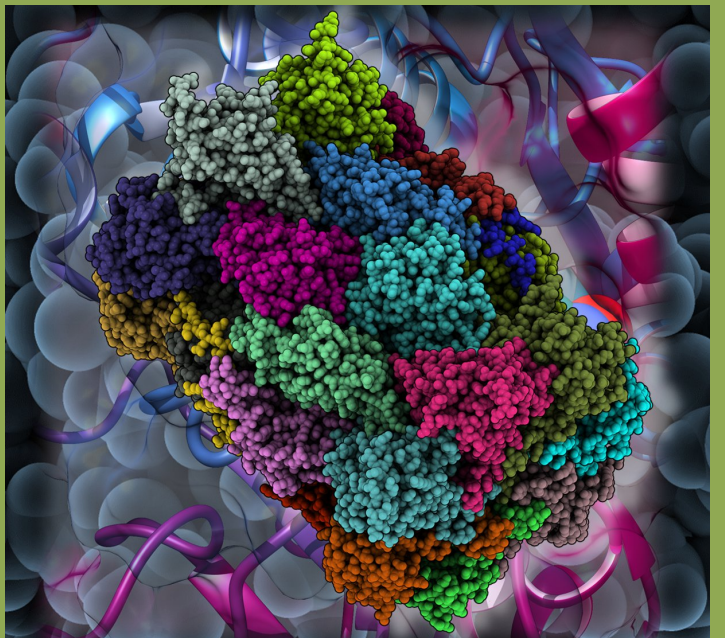


QM/MM STUDIES ON THE INHIBITION OF HUMAN 20S PROTEASOME

THE ROLE OF ELECTROSTATIC EFFECTS IN BIOCATALYSIS

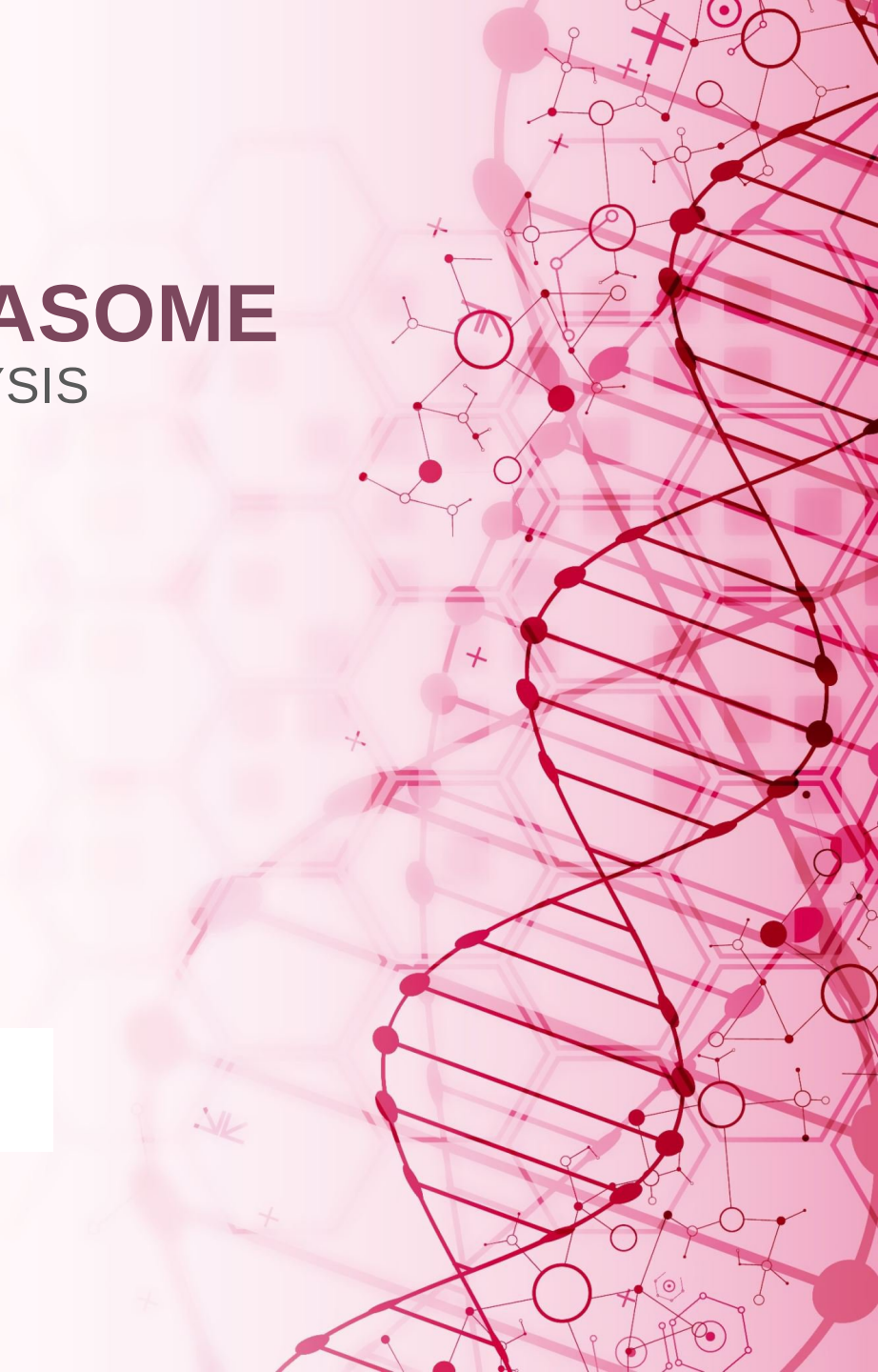


UJI UNIVERSITAT
JAUME I

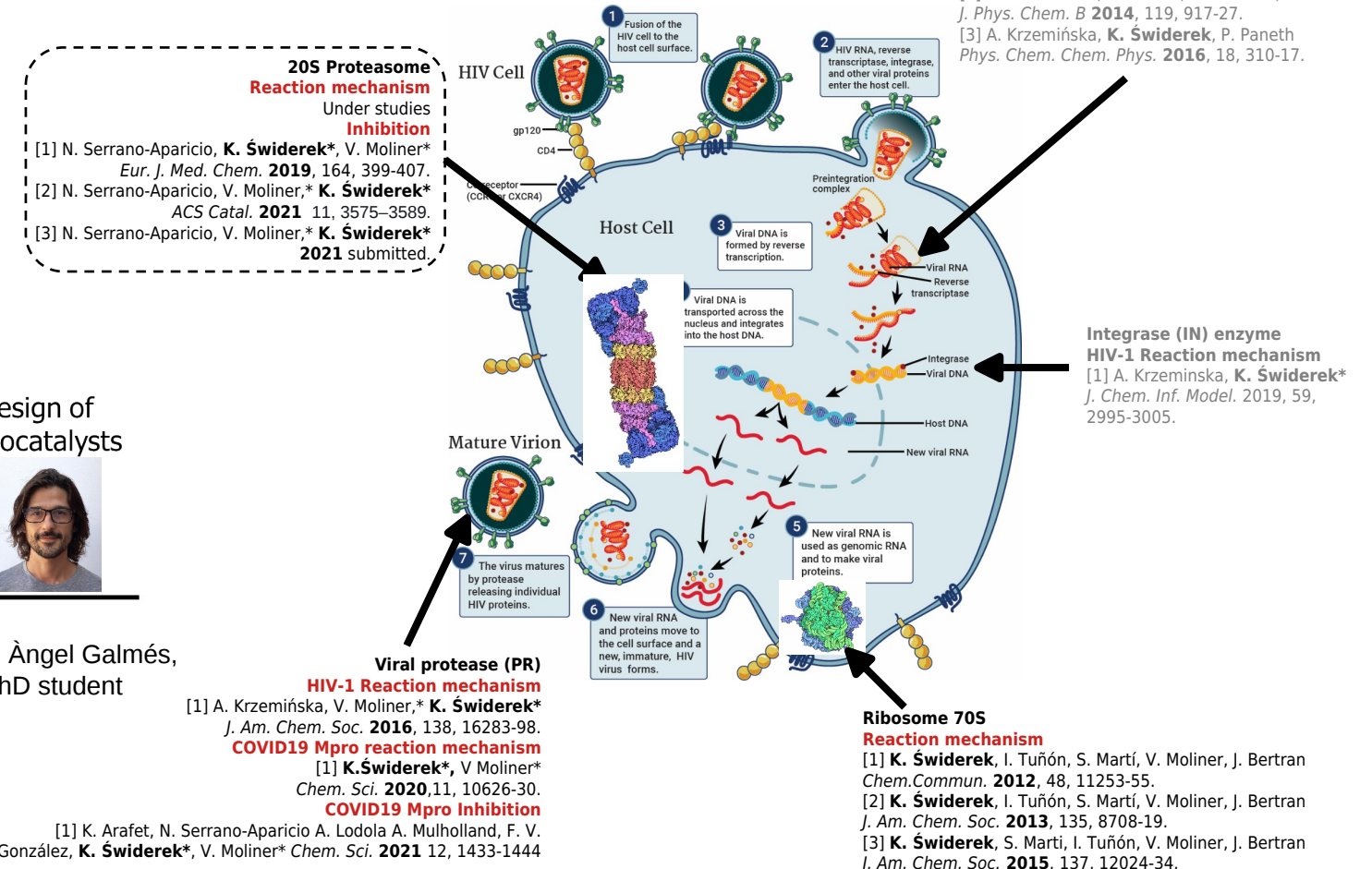
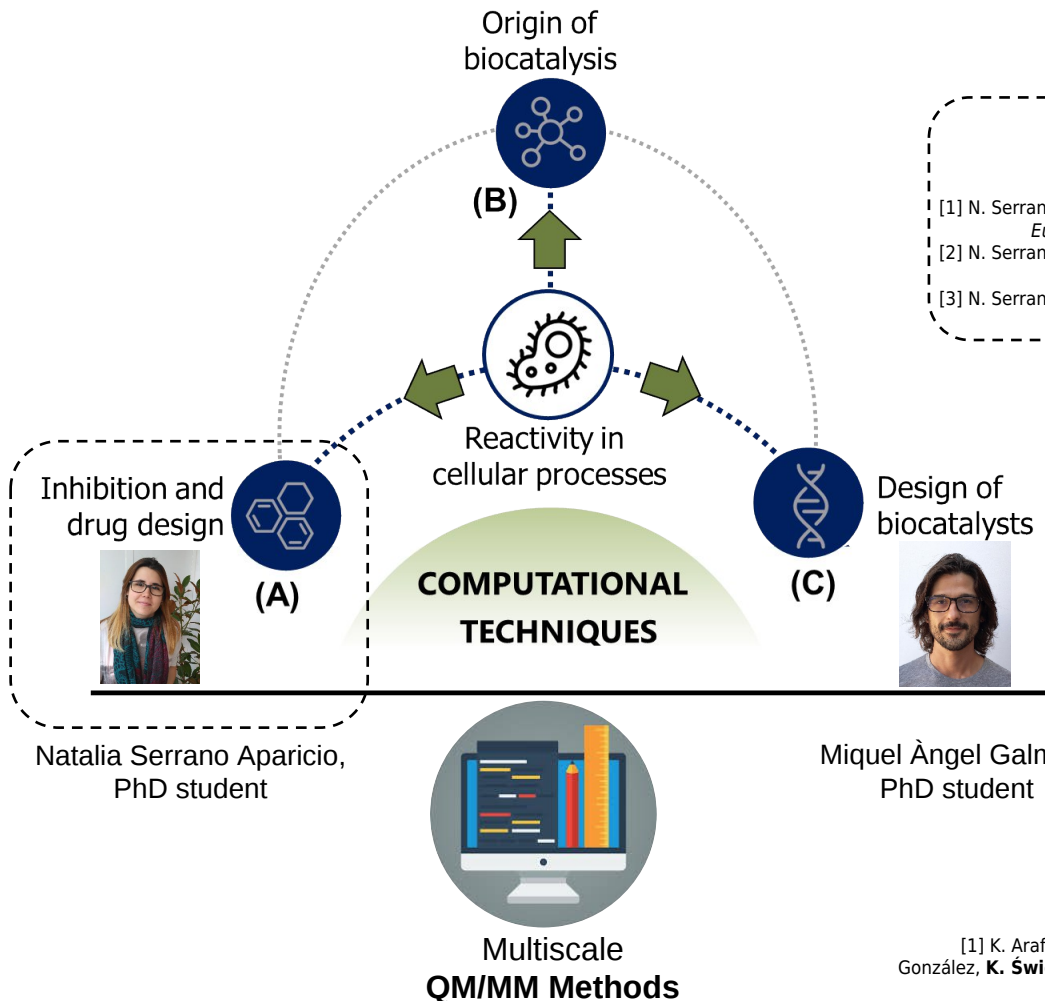
Katarzyna Świderek
Biocomp group, Universitat Jaume I, Spain

BioComp group <http://www.biocomp.uji.es/>

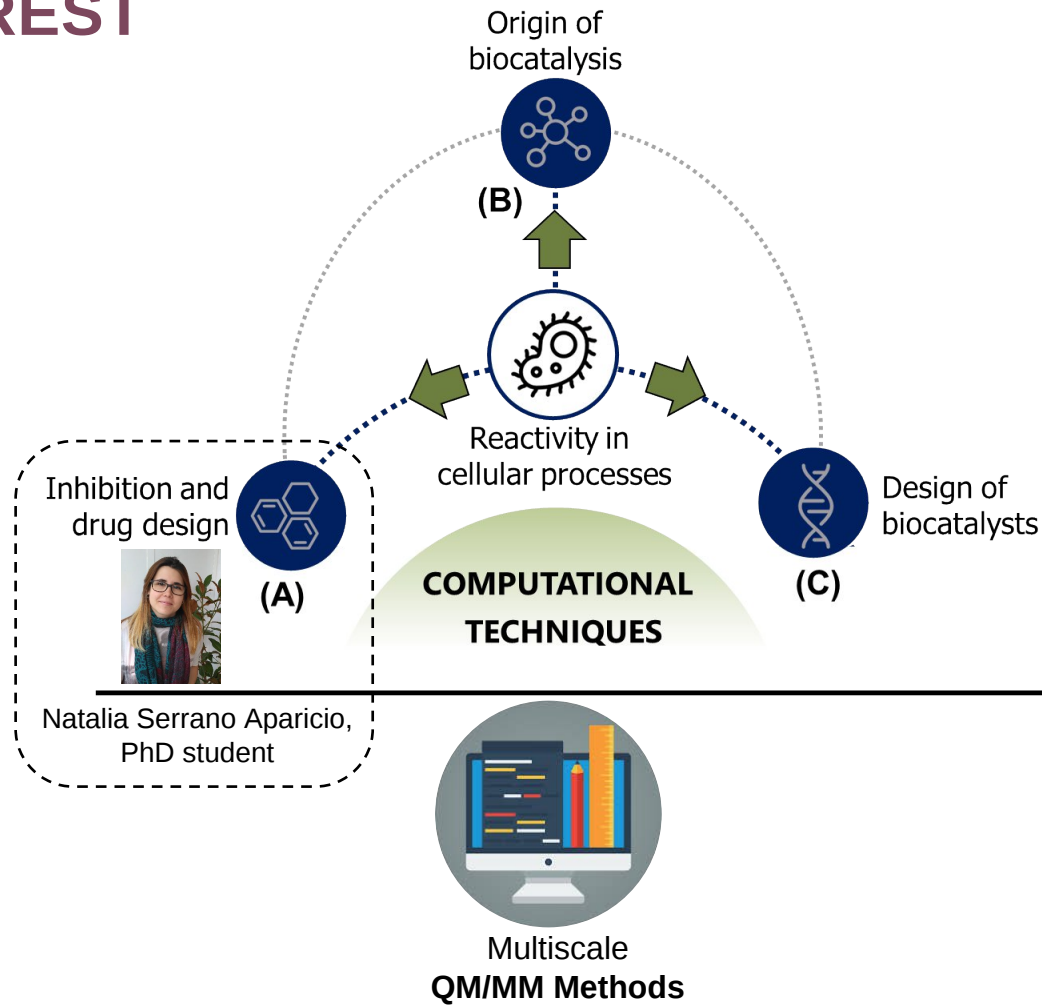
StopProt project <http://www.biocomp.uji.es/swiderek/home.html>



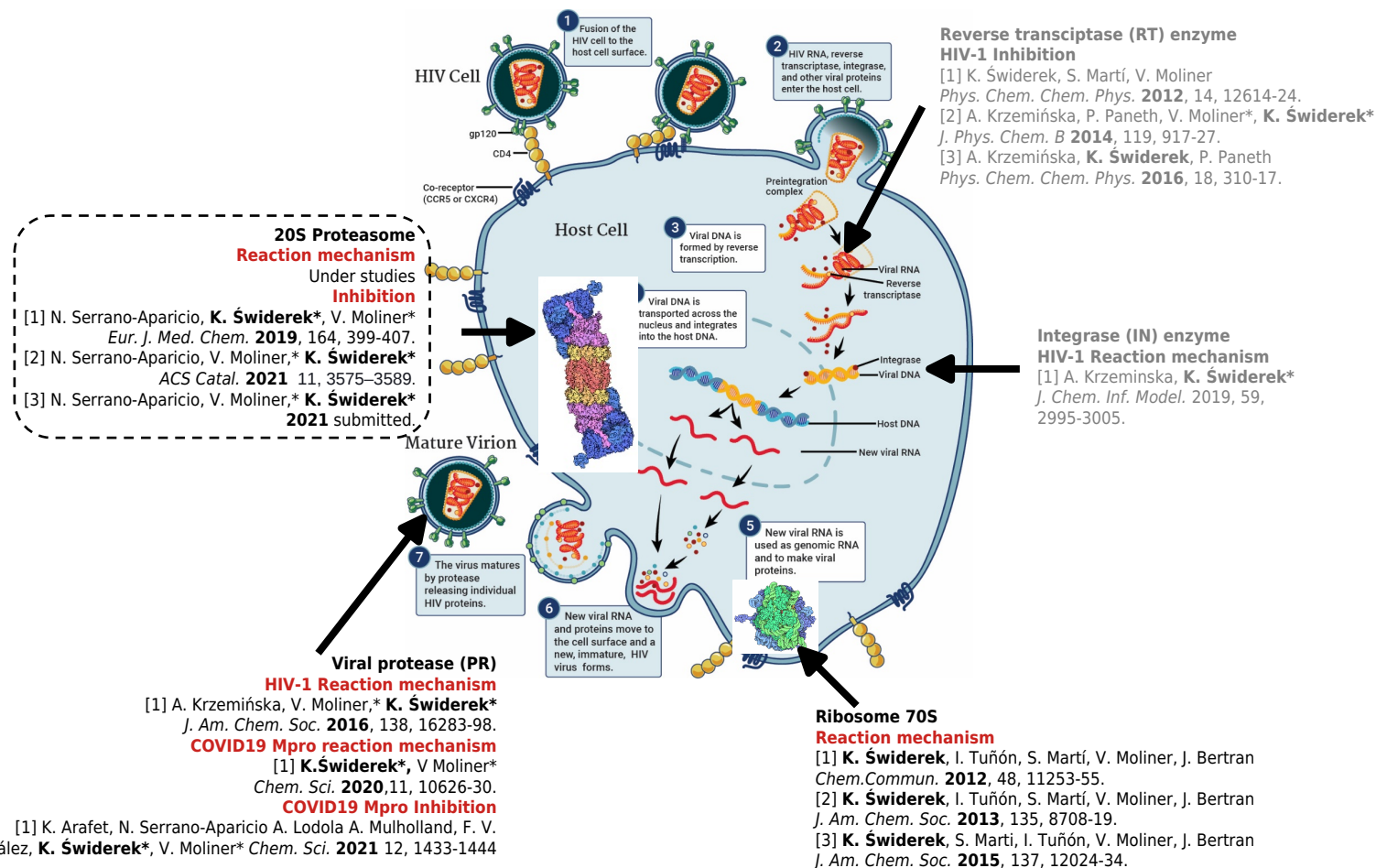
RESEARCH INTEREST



RESEARCH INTEREST



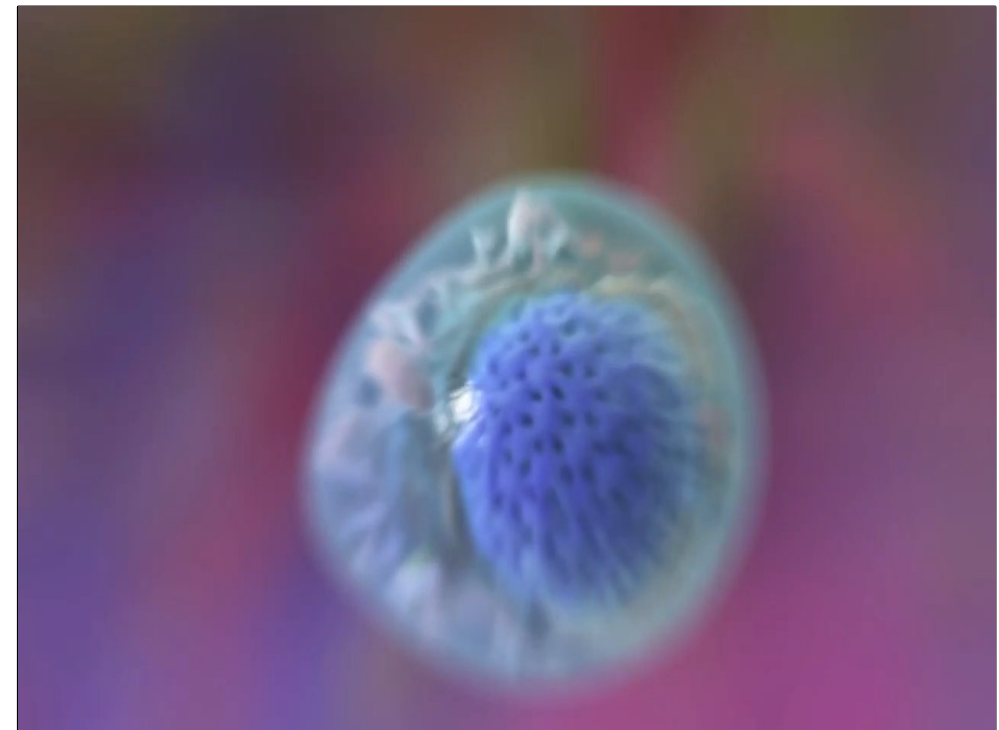
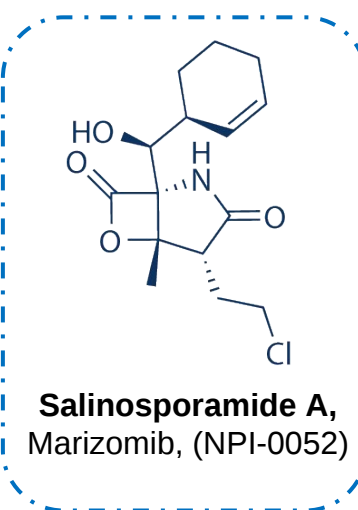
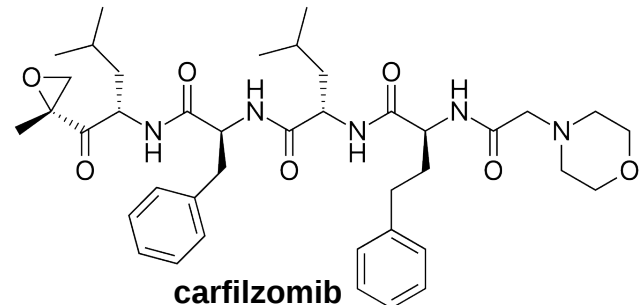
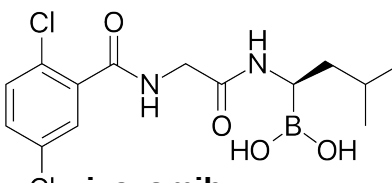
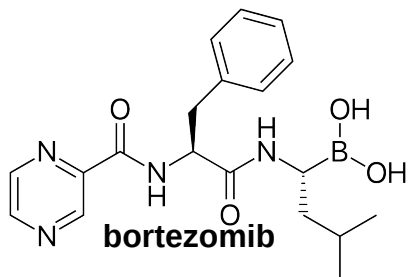
RESEARCH INTEREST



20S PROTEASOME – ROLE AND CHARACTERISTIC

Designed covalent inhibitors can be classified based on the nature of the electrophilic warhead employed to interact with Thr1. Therefore, using this rule, **eight groups** of covalent inhibitors can be distinguished such as **aldehydes**, **boronates**, **epoxyketones**, **α -ketoaldehydes**, **vinyl sulfones**, **syrbactins**, **bacteria-specific oxazol-2-ones**, and **β -lactones**.

However, inhibitory studies have led to just three peptide-like compounds approved by the Food and Drug Administration (FDA) for cancer treatment: two peptide boronate inhibitors, **bortezomib** (VELCADE) and **ixazomib** (NINLARO), and the peptide epoxyketone inhibitor **carfilzomib** (KYPROLIS).



Medi-mation.com

The Nobel Prize in Chemistry 2004 : A. Ciechanover; A. Hershko, I. Rose "for the discovery of ubiquitin-mediated protein degradation."

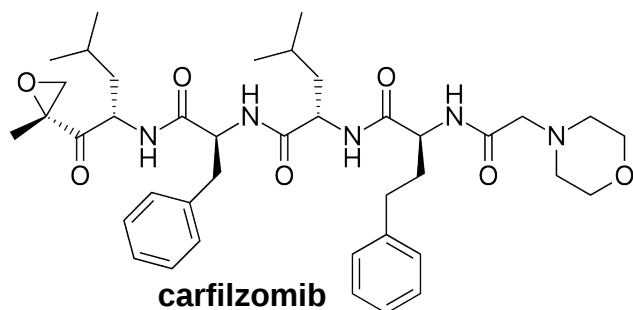
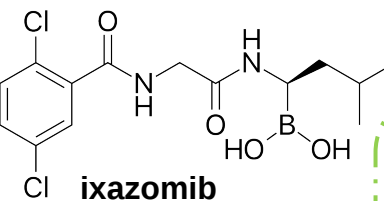
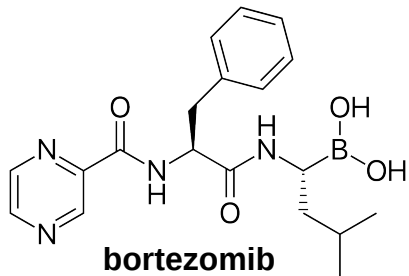
Huber, E.H. et al. Cell. 2012, 148, 727-738.

Saha, A and Warshel, A. PNAS 2021 118 just accepted.

20S PROTEASOME – ROLE AND CHARACTERISTIC

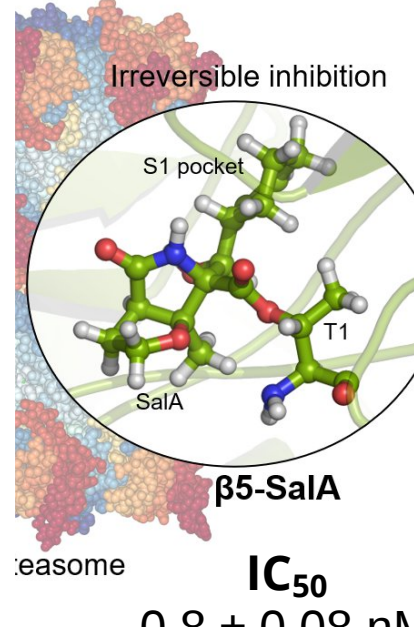
They can be classified based on the nature of the electrophilic warhead employed to interact with Thr1. Therefore, using this rule, **eight groups** of covalent inhibitors can be distinguished such as **aldehydes**, **boronates**, **epoxyketones**, **α -ketoaldehydes**, **vinyl sulfones**, **syrbactins**, **bacteria-specific oxazol-2-ones**, and **β -lactones**.

However, inhibitory studies have led to just three peptide-like compounds approved by the Food and Drug Administration (FDA) for cancer treatment: two peptide boronate inhibitors, **bortezomib** (VELCADE) and **ixazomib** (NINLARO), and the peptide epoxyketone inhibitor **carfilzomib** (KYPROLIS).



**Salinosporamide A,
Marizomib, (NPI-0052)**

COVALENT INHIBITION OF PROTEASOME 20S



Groll, M. et al. *J. Am. Chem. Soc.* **2006**, 128, 5136-5141.



salinosporamide A
(SalA)

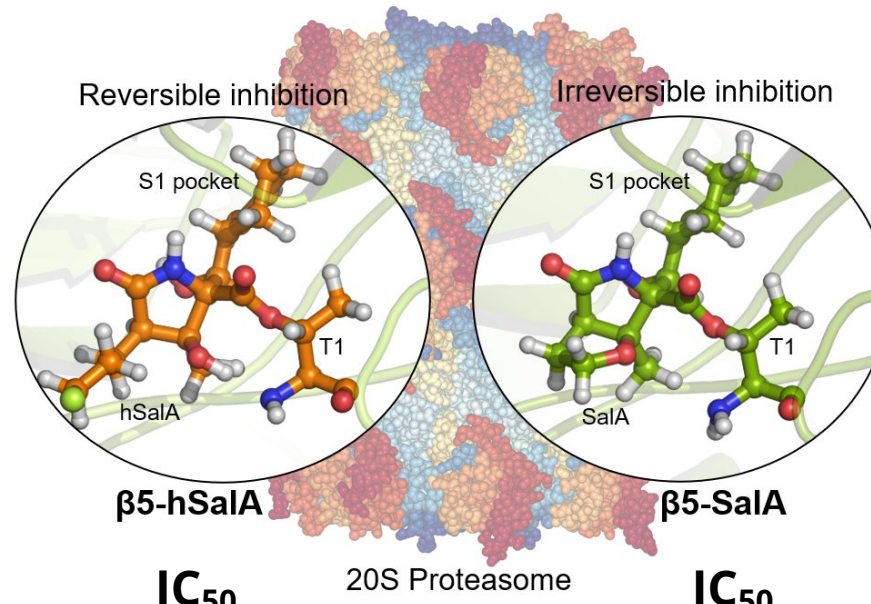
COVALENT INHIBITION OF PROTEASOME 20S

Nguyen, H. et al. *J. Org. Chem.* **2011**, 76, 2–12.
Groll, M. et al. *Marine Drugs* **2018**, 16, 240.

Groll, M. et al. *J. Am. Chem. Soc.* **2006**, 128, 5136-5141.



homo-salinosporamide A
(hSalA)



salinosporamide A
(SalA)

What is the origin of different inhibition character of SalA and hSalA?

QM/MM MD METHODS

VTST Rate constant

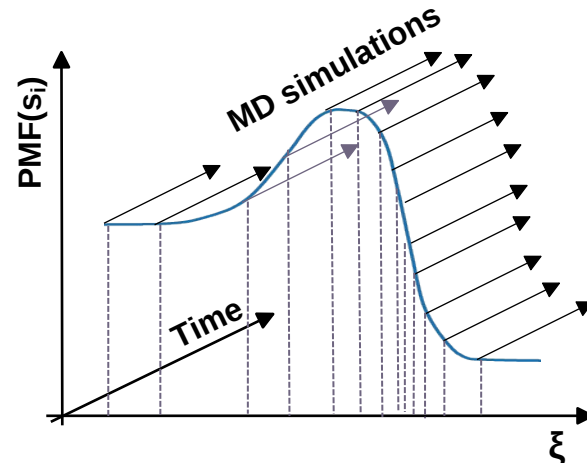


WHAM (Weighted Histogram Analysis Method)



Umbrella Sampling (US)

To study an enzyme catalyzed reaction within the substrate-environment equilibrium approximation:
Transition State Theory (TST)

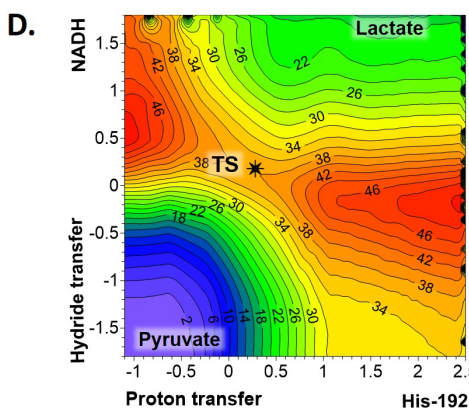
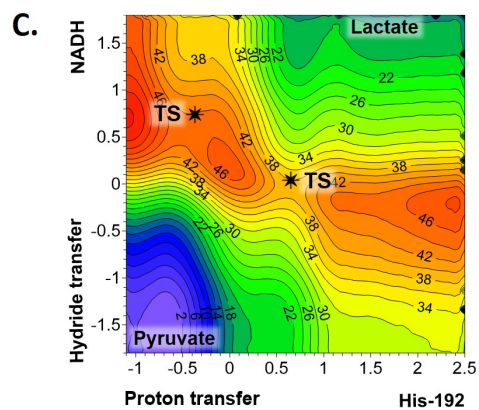
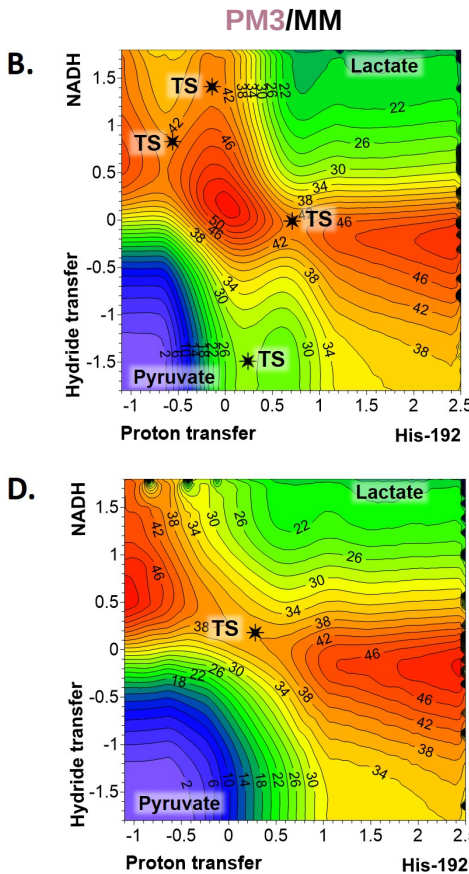
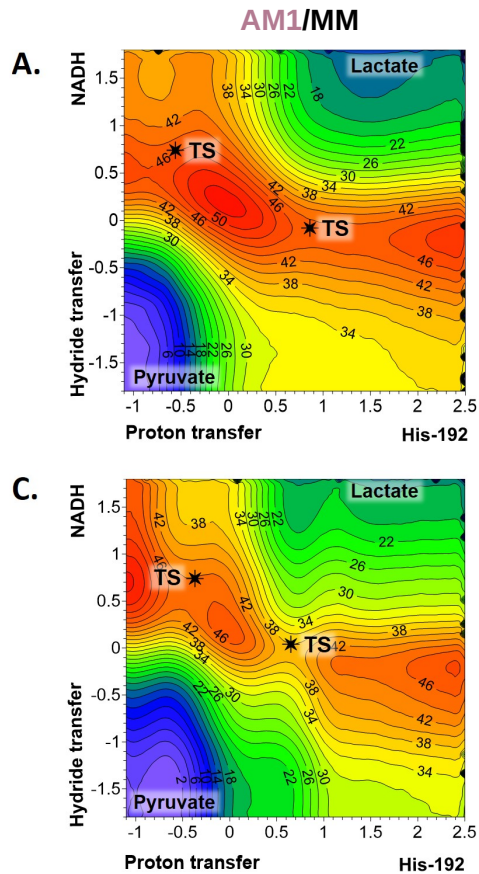


Biased QM/MM (**AM1/MM**) MD simulation along a distinguished reaction coordinate : **Potential Mean Force**

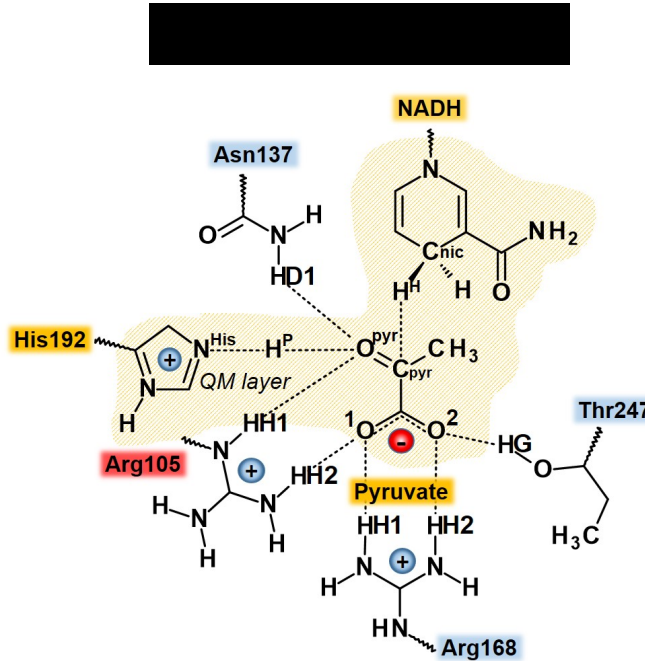
Spline correction method (M06-2X:AM1/MM)

QM/MM MD METHODS

PMF computed at semiempirical level (SE/MM)

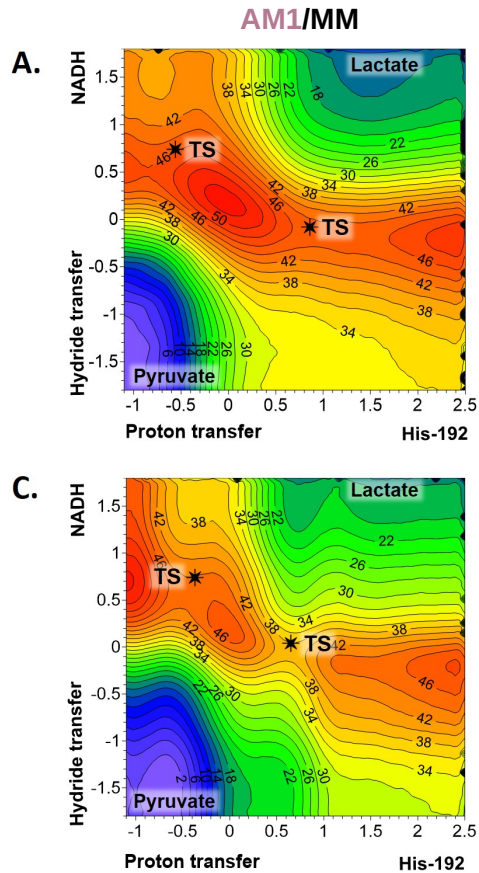


Spline correction method (M06-2X/MM)



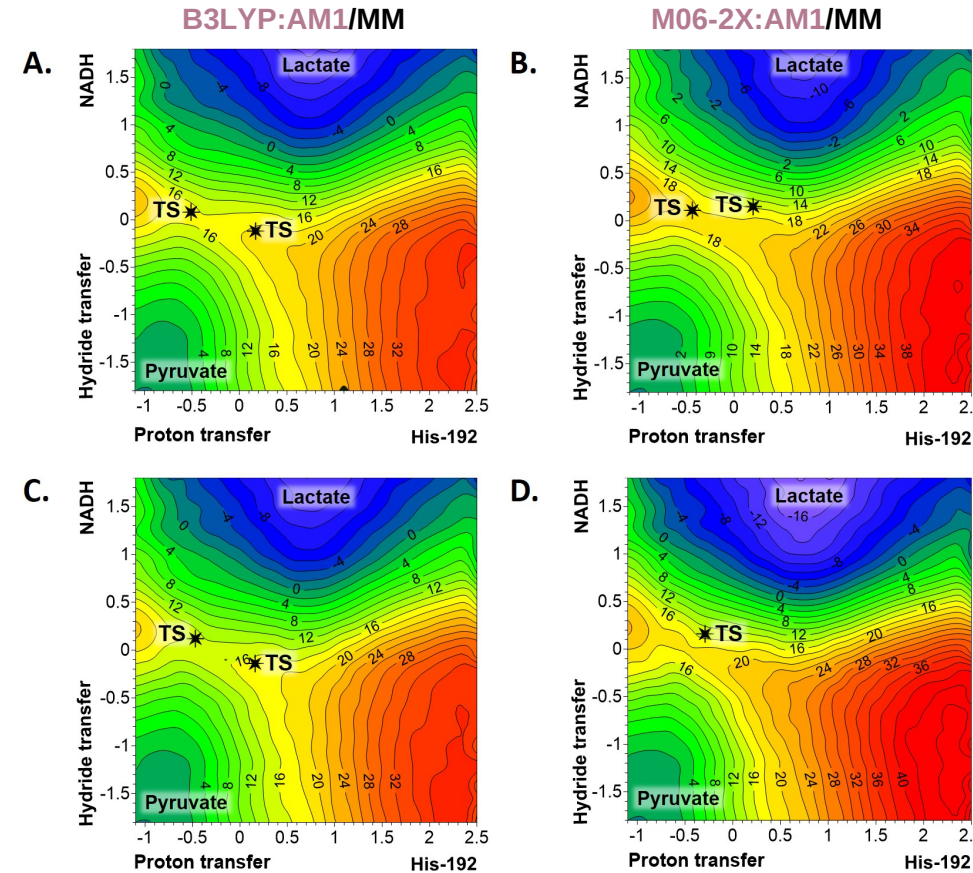
QM/MM MD METHODS

PMF computed at semiempirical level (SE/MM)



Spline correction method (M06-2X/MM)

Corrected PMF at M06-2X/6-31+G(d,p) level



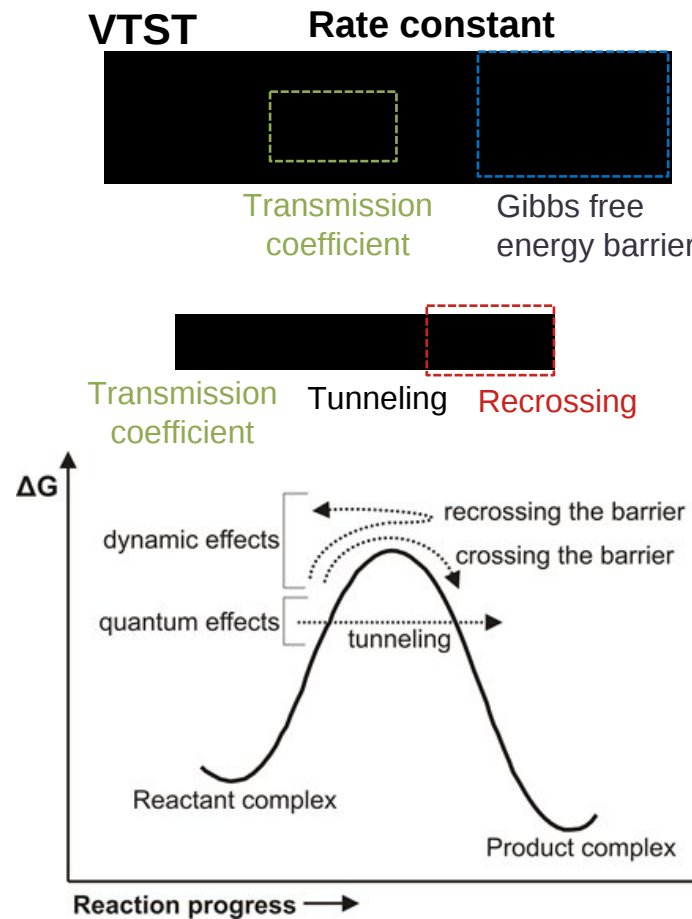
PDDG/MM

RM1/MM

mPW1PW91:AM1/MM

MP2:AM1/MM

QM/MM MD METHODS



Equilibrium and Kinetic Isotope Effects

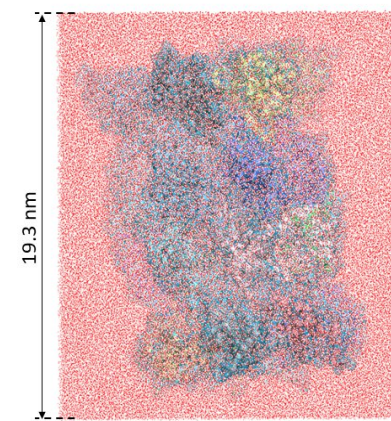
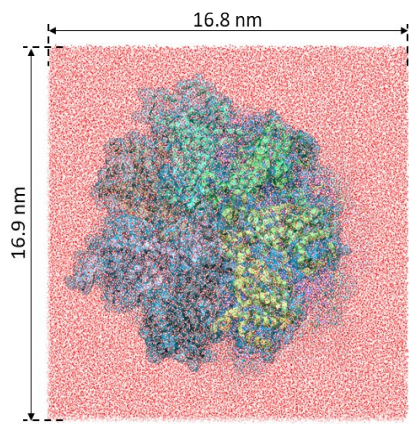
$$IE = \frac{\left(\frac{Q_a}{Q_b}\right)_L e^{-1/RT(\Delta ZPE_L - \Delta ZPE_H)}}{\left(\frac{Q_a}{Q_b}\right)_H}$$

Translational, rotational and vibrational contribution

$$KIE = KIE^{QC} \times \frac{\gamma_L}{\gamma_H} \times \frac{K_L}{K_H} = KIE^{QC} \times KIE^\gamma \times KIE^K$$

QM/MM MD METHODS

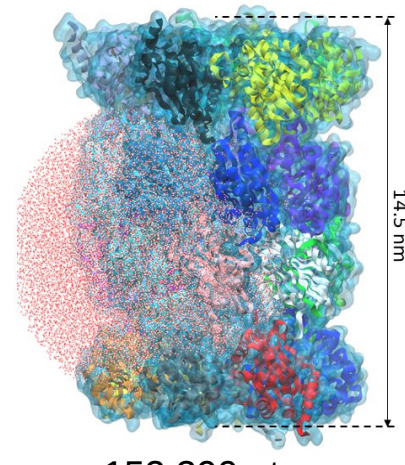
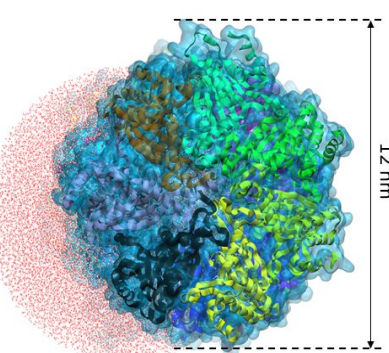
Model for MM MD simulations



527 831 atoms in total

Model for QM/MM MD simulations

60 Å water sphere centred on Thr1



152 390 atoms

ChemComm

FEATURE ARTICLE



[View Article Online](#)
[View Journal](#) | [View Issue](#)



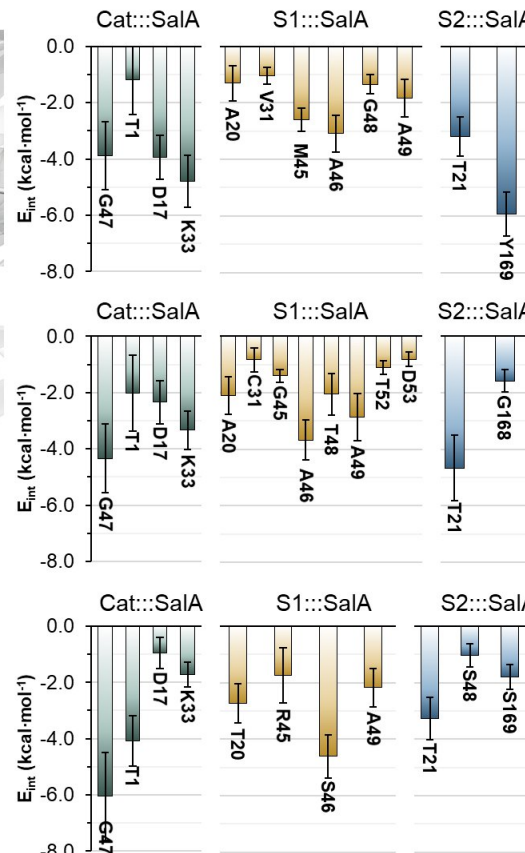
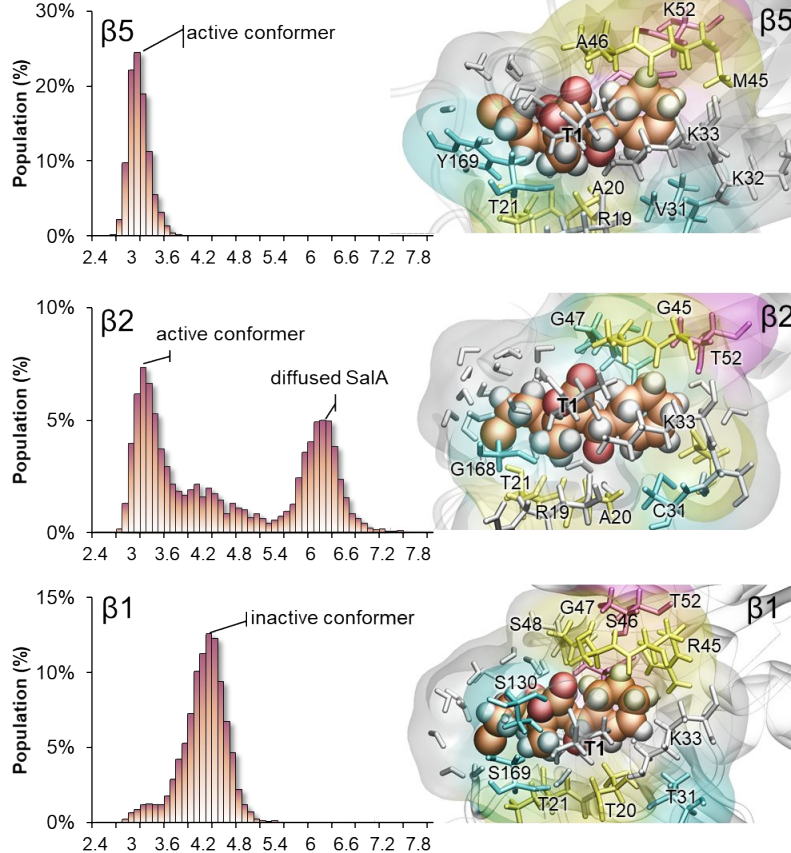
Cite this: *Chem. Commun.*, 2017,
53, 284

Computational tools for the evaluation of laboratory-engineered biocatalysts

Adrian Romero-Rivera,^a Marc Garcia-Borràs^b and Silvia Osuna^{*a}

Computational strategy	Accounting for:				Useful for studying:					Computational cost	Computational strategy	Key examples	
	QM	MM	Active site	Whole enzyme	Protein flexibility	Enantioselectivity/ Stereoselectivity	Substrate scope	Reaction mechanism	Conformational dynamics				
<i>Cluster model</i>	✓	✗	✓	✗	✗	✓	✓	✓	✗	✗	+	89, 90	91-93
<i>Theozyme</i>	✓	✗	✓	✗	✗	✓	✓	✓	✗	✗	+	84-87	88
<i>QM/MM</i>	✓	✓	✓	✓	✗	✓	✓	✓	✗	✗	++	94-96	97, 98
<i>QM/MM-MD</i>	✓	✓	✓	✓	✓	✓	✓	✓	✗	✗	++++	99	99
<i>EVB</i>	✓	✓	✓	✓	✗	✓	✓	✓	✗	✗	++	100-102	103, 104
<i>MD</i>	✗	✓	✓	✓	✓	✓	✓	✗	✓	✓	+	105-108	109, 110
<i>MC</i>	✗	✓	✓	✓	✓	✓	✓	✗	✓	✓	+	111, 112	113

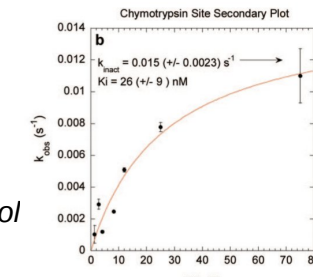
RECOGNITION STEP of SalA



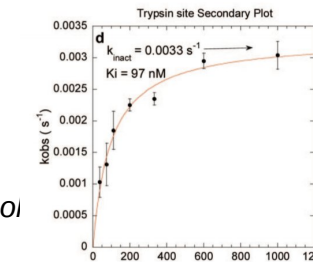
$$\begin{aligned} K_i &= 23 \pm nM^{(a)} \\ IC_{50} &= 2.0 \pm 0.3 nM^{(a)} \\ IC_{50} &= 0.8 \pm 0.08^{(b)} \\ E_{int} &= -54.1 \pm 3.1 \text{ kcal}\cdot\text{mol} \end{aligned}$$

Experimental data

$$k_{inact} = 0.015 \text{ s}^{-1}^{(b)}$$

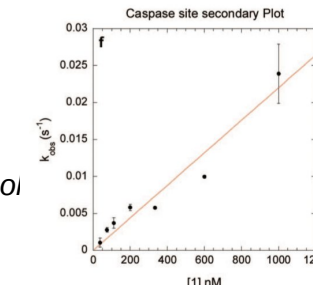


$$\begin{aligned} K_i &= 97 \pm nM^{(a)} \\ IC_{50} &= 59 \pm 1 nM^{(a)} \\ IC_{50} &= 39 \pm 7^{(b)} \\ E_{int} &= -45.8 \pm 3.3 \text{ kcal}\cdot\text{mol} \end{aligned}$$



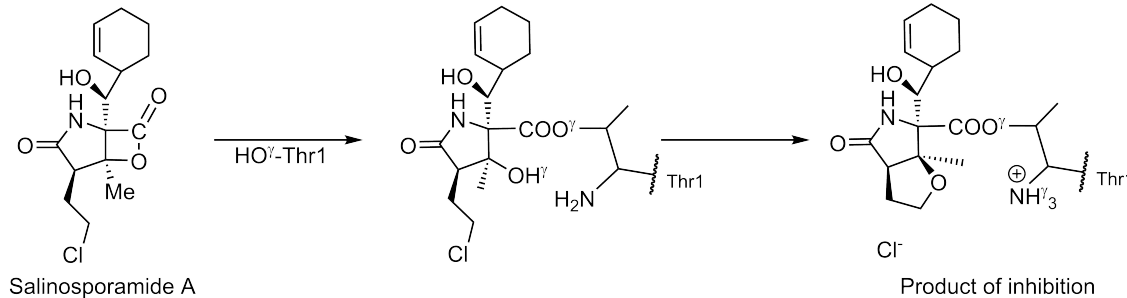
$$k_{inact} = 0.0033 \text{ s}^{-1}^{(b)}$$

$$\begin{aligned} K_i &> 1000 nM^{(a)} \\ IC_{50} &= 2600 \pm 200 nM^{(a)} \\ IC_{50} &= 111 \pm 22^{(b)} \\ E_{int} &= -42.6 \pm 2.8 \text{ kcal}\cdot\text{mol} \end{aligned}$$



$$k_{inact} >> 0.02 \text{ s}^{-1}^{(b)}$$

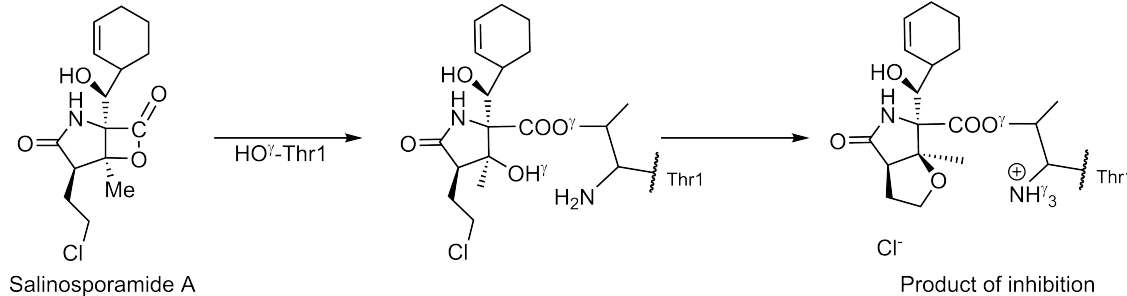
20S PROTEASOME INHIBITION WITH SalA



Groll, M. et al. *J. Am. Chem. Soc.* **2006**, 128, 5136-5141
Macherla, V.R. et al. *J. Med. Chem.* **2005**, 48, 3684-3687

SalA-assisted mechanism

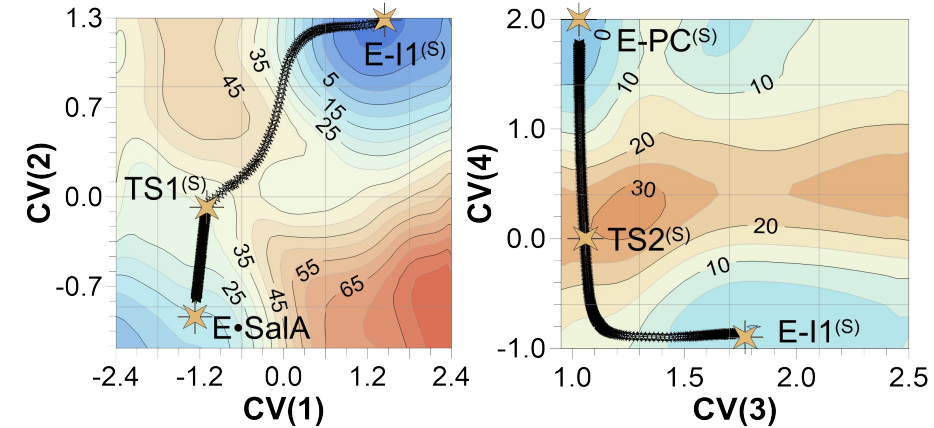
20S PROTEASOME INHIBITION WITH SalA⁺



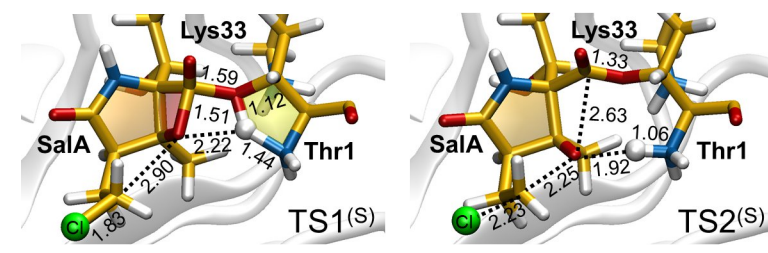
Groll, M. et al. *J. Am. Chem. Soc.* **2006**, 128, 5136-5141
Macherla, V.R. et al. *J. Med. Chem.* **2005**, 48, 3684-3687

SalA-assisted mechanism

2D-PMF M06-2X:AM1/MM

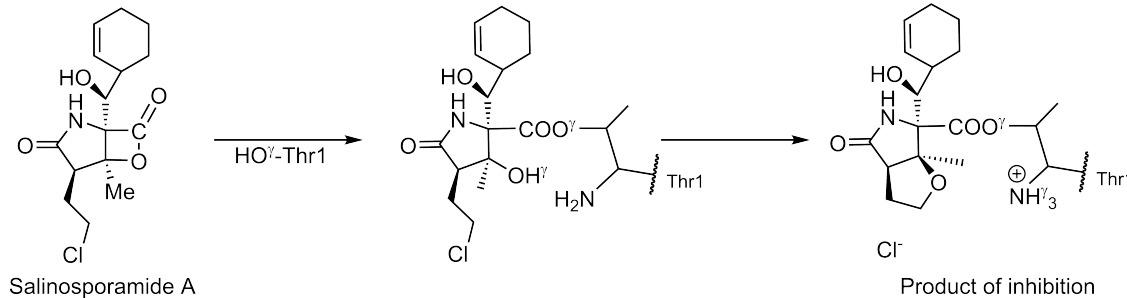


Applied collective variables are defined as follow:
 $\text{CV}(1) = d(\text{O}^\gamma\text{Thr1}-\text{H}^\gamma\text{Thr1}) - d(\text{H}^\gamma\text{Thr1}-\text{O}^2\text{SalA})$, $\text{CV}(2) = d(\text{O}^2\text{SalA}-\text{C}1\text{SalA}) - d(\text{O}^\gamma\text{Thr1}-\text{C}1\text{SalA})$,
 $\text{CV}(3) = d(\text{H}^\gamma\text{Thr1}-\text{N}^\gamma\text{Thr1})$, $\text{CV}(4) = d(\text{O}^2\text{SalA}-\text{C}3\text{SalA}) - (\text{C}3\text{SalA}-\text{Cl})$,



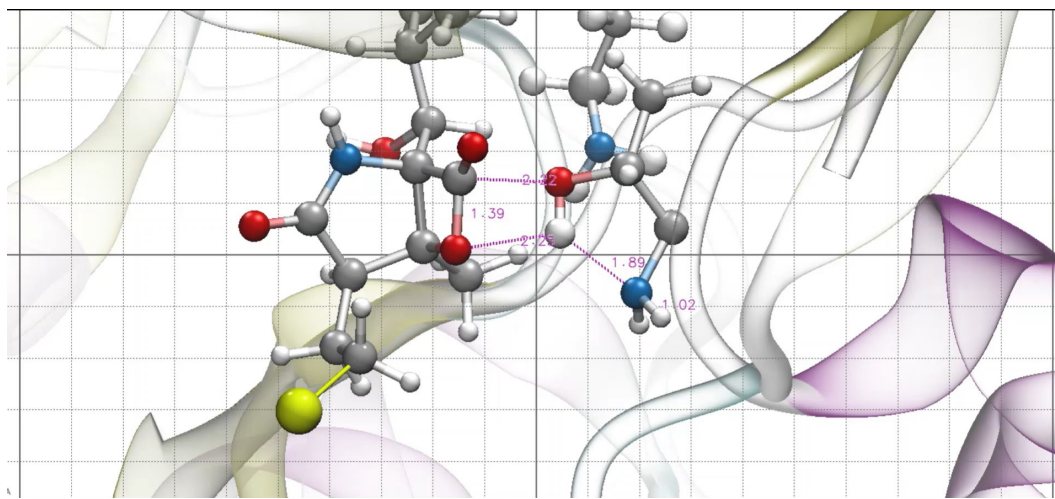
TS structures at M06-2X/MM

20S PROTEASOME INHIBITION WITH SalA^{1A}

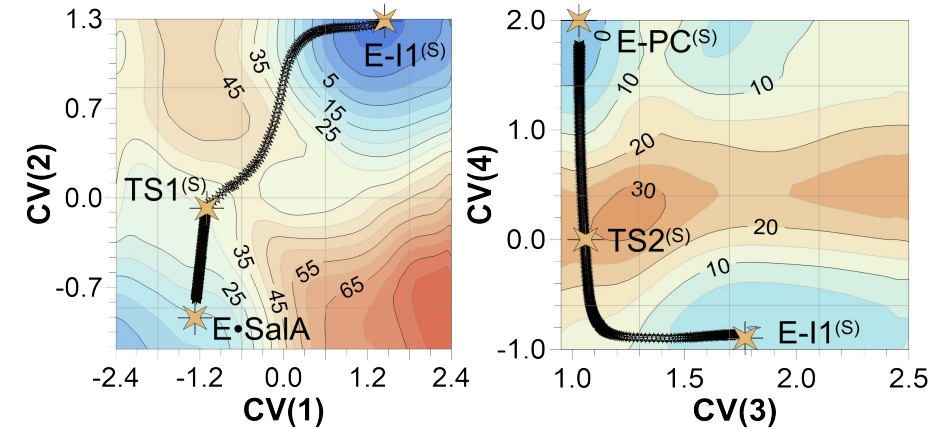


Groll, M. et al. *J. Am. Chem. Soc.* **2006**, 128, 5136-5141
Macherla, V.R. et al. *J. Med. Chem.* **2005**, 48, 3684-3687

SalA-assisted mechanism

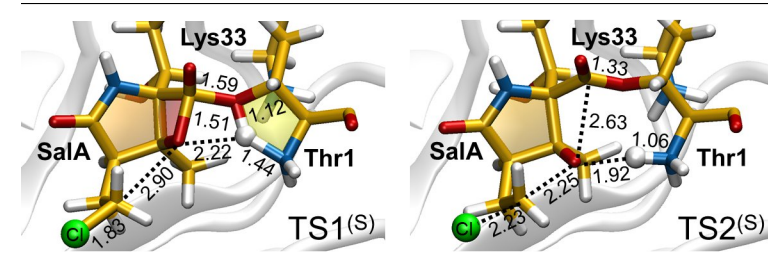


2D-PMF M06-2X:AM1/MM



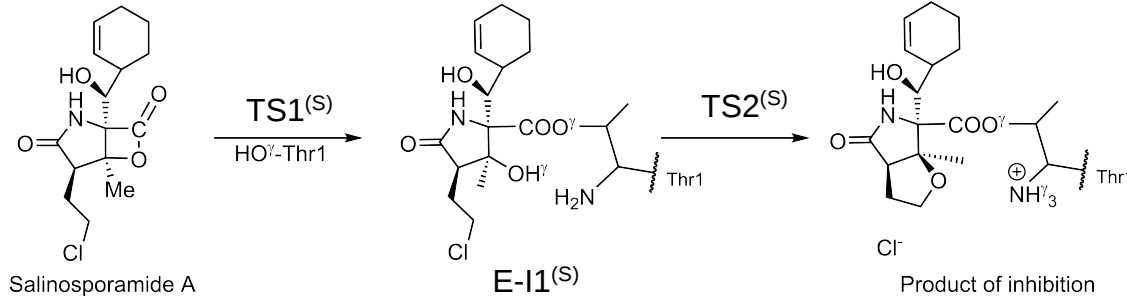
Applied collective variables are defined as follow:

$$\begin{aligned} \text{CV}(1) &= d(\text{O}^\gamma\text{Thr1}-\text{H}^\gamma\text{Thr1}) - d(\text{H}^\gamma\text{Thr1}-\text{O}^2\text{SalA}), \quad \text{CV}(2) = d(\text{O}^2\text{SalA}-\text{C}1\text{SalA}) - d(\text{O}^\gamma\text{Thr1}-\text{C}1\text{SalA}), \\ \text{CV}(3) &= d(\text{H}^\gamma\text{Thr1}-\text{N}^\gamma\text{Thr1}), \quad \text{CV}(4) = d(\text{O}^2\text{SalA}-\text{C}3\text{SalA}) - (\text{C}3\text{SalA}-\text{Cl}), \end{aligned}$$



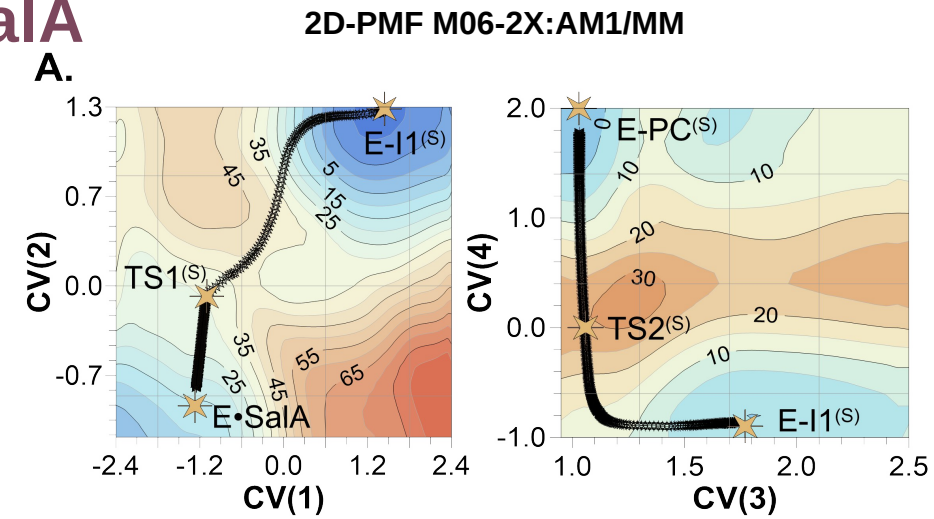
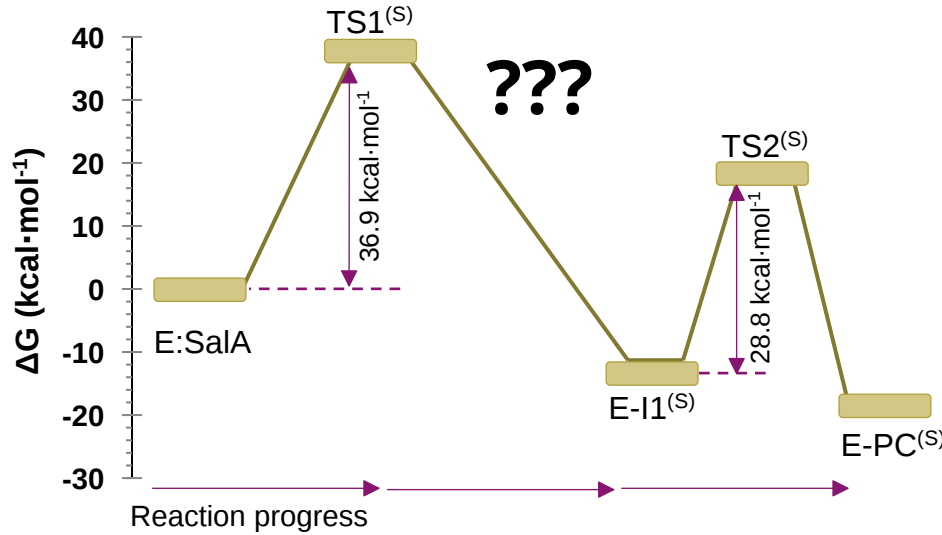
TS structures at M06-2X/MM

20S PROTEASOME INHIBITION WITH SalA



Groll, M. et al. *J. Am. Chem. Soc.* **2006**, 128, 5136-5141
Macherla, V.R. et al. *J. Med. Chem.* **2005**, 48, 3684-3687

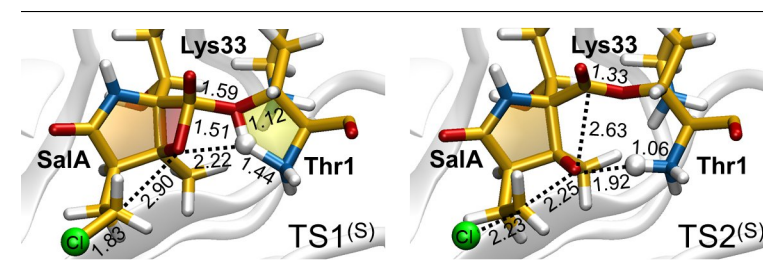
SalA-assisted mechanism



Applied collective variables are defined as follow:

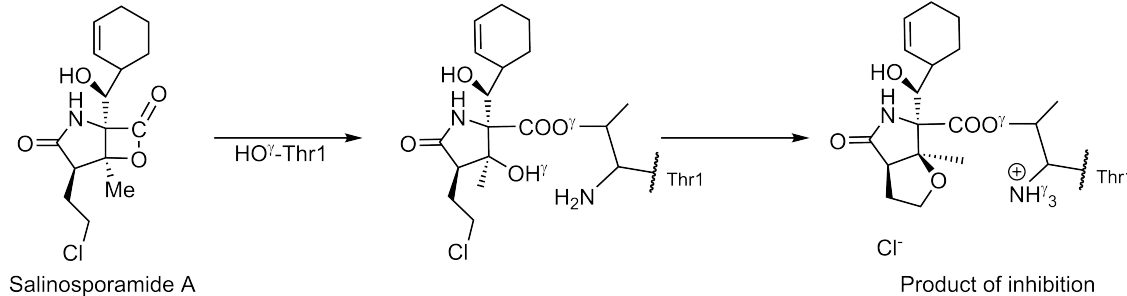
$\text{CV}(1) = d(\text{O}^{\gamma}\text{Thr1}-\text{H}^{\gamma}\text{Thr1}) - d(\text{H}^{\gamma}\text{Thr1}-\text{O}^{\alpha}\text{SalA})$, $\text{CV}(2) = d(\text{O}^{\alpha}\text{SalA}-\text{C}^{\beta}\text{SalA}) - d(\text{O}^{\gamma}\text{Thr1}-\text{C}^{\beta}\text{SalA})$,

$\text{CV}(3) = d(\text{H}^{\gamma}\text{Thr1}-\text{N}^{\gamma}\text{Thr1})$, $\text{CV}(4) = d(\text{O}^{\alpha}\text{SalA}-\text{C}^{\delta}\text{SalA}) - (\text{C}^{\beta}\text{SalA}-\text{Cl})$,



TS structures at M06-2X/MM

20S PROTEASOME INHIBITION WITH SalA



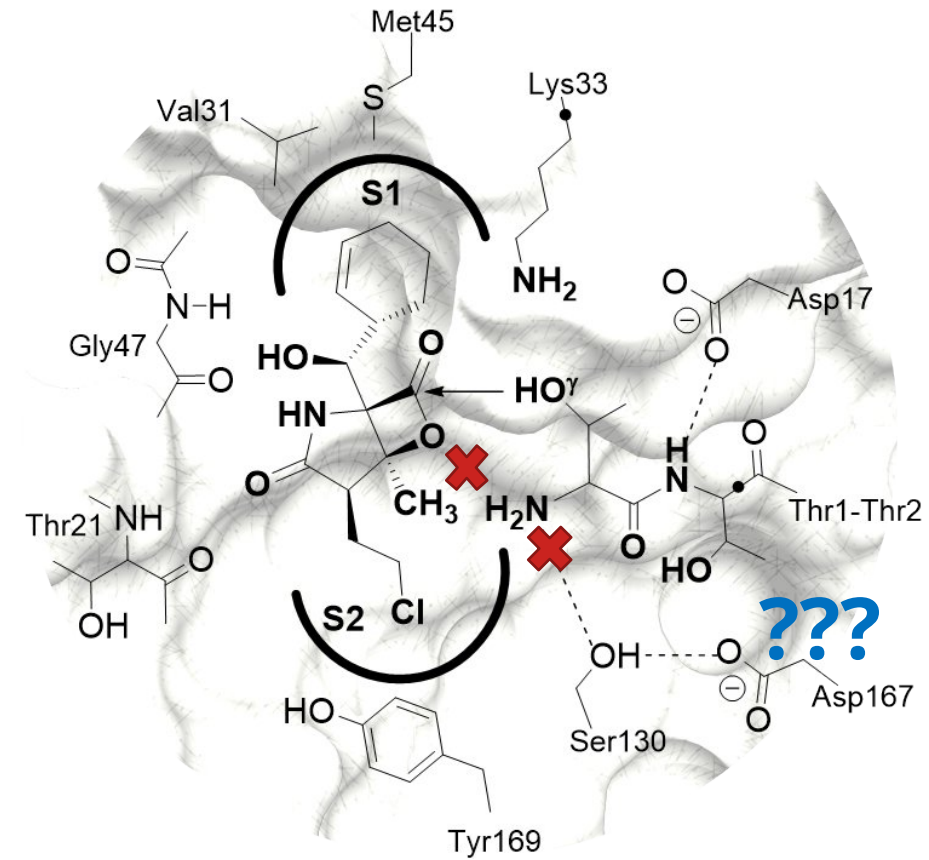
Groll, M. et al. *J. Am. Chem. Soc.* **2006**, 128, 5136-5141
Macherla, V.R. et al. *J. Med. Chem.* **2005**, 48, 3684-3687

SalA-assisted mechanism

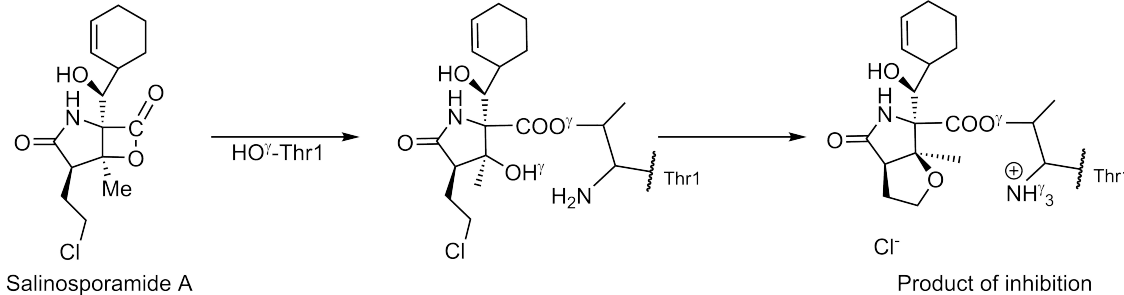
„X-ray data on the $\beta 5\text{-D167N}$ mutant indicate that the $\beta 5$ propeptide is hydrolysed, but due to reorientation of Ser129OH, the interaction with Asn166- O^δ is disrupted”

Huber E.M. et al. *Nat. Commun.* **2016**, 7, 10900

Active site of the $\beta 5$ subunit



20S PROTEASOME INHIBITION WITH SalA

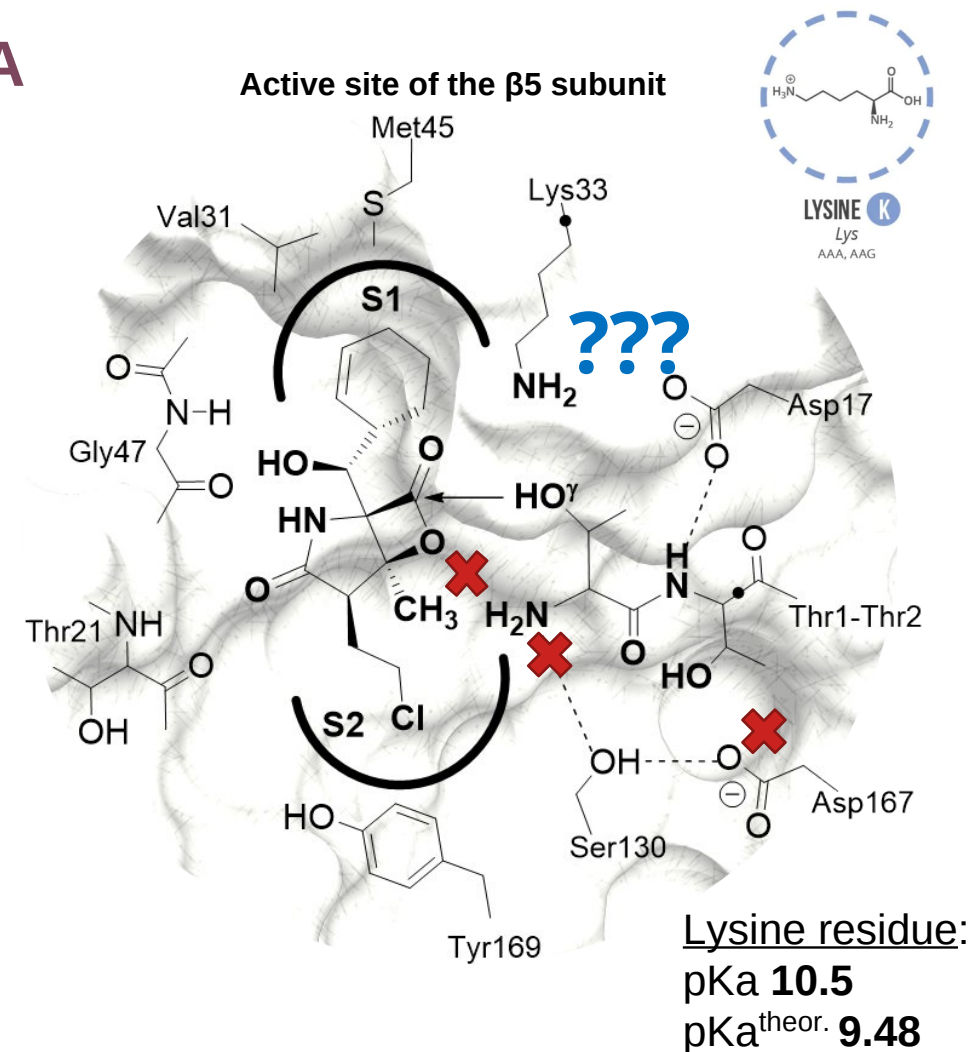


Groll, M. et al. *J. Am. Chem. Soc.* **2006**, 128, 5136-5141
Macherla, V.R. et al. *J. Med. Chem.* **2005**, 48, 3684-3687

SalA-assisted mechanism

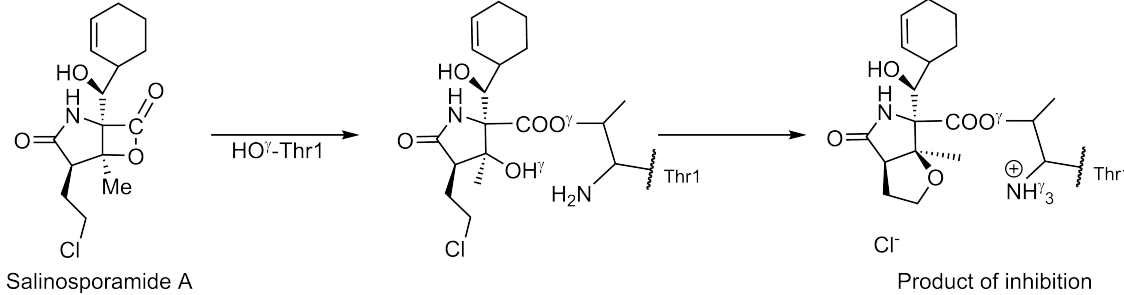
„The proof for the key function of Lys33 was obtained from the β 5-K33A mutant, with the propeptide expressed separately from the main subunit. The Thr1 N terminus of this mutant is not blocked by the propeptide, yet its catalytic activity is reduced by ~83%.”

Huber E.M. et al. *Nat. Commun.* **2016**, 7, 10900



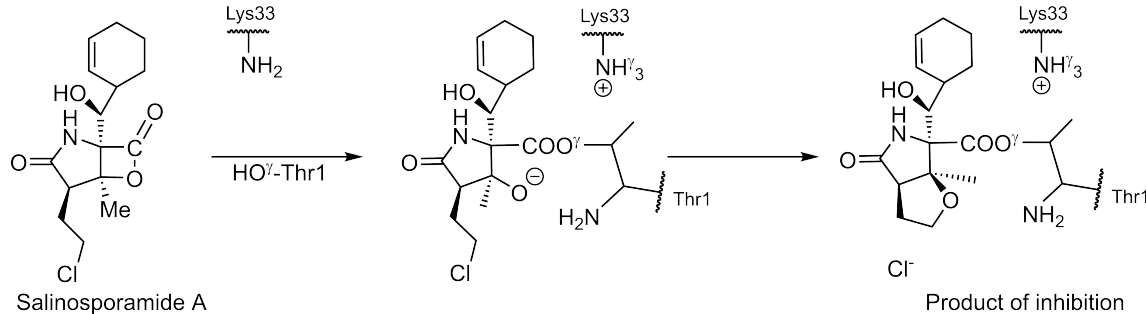
Lysine residue:
pKa **10.5**
pKa^{theor.} **9.48**

20S PROTEASOME INHIBITION WITH SalA



Groll, M. et al. *J. Am. Chem. Soc.* **2006**, 128, 5136-5141
Macherla, V.R. et al. *J. Med. Chem.* **2005**, 48, 3684-3687

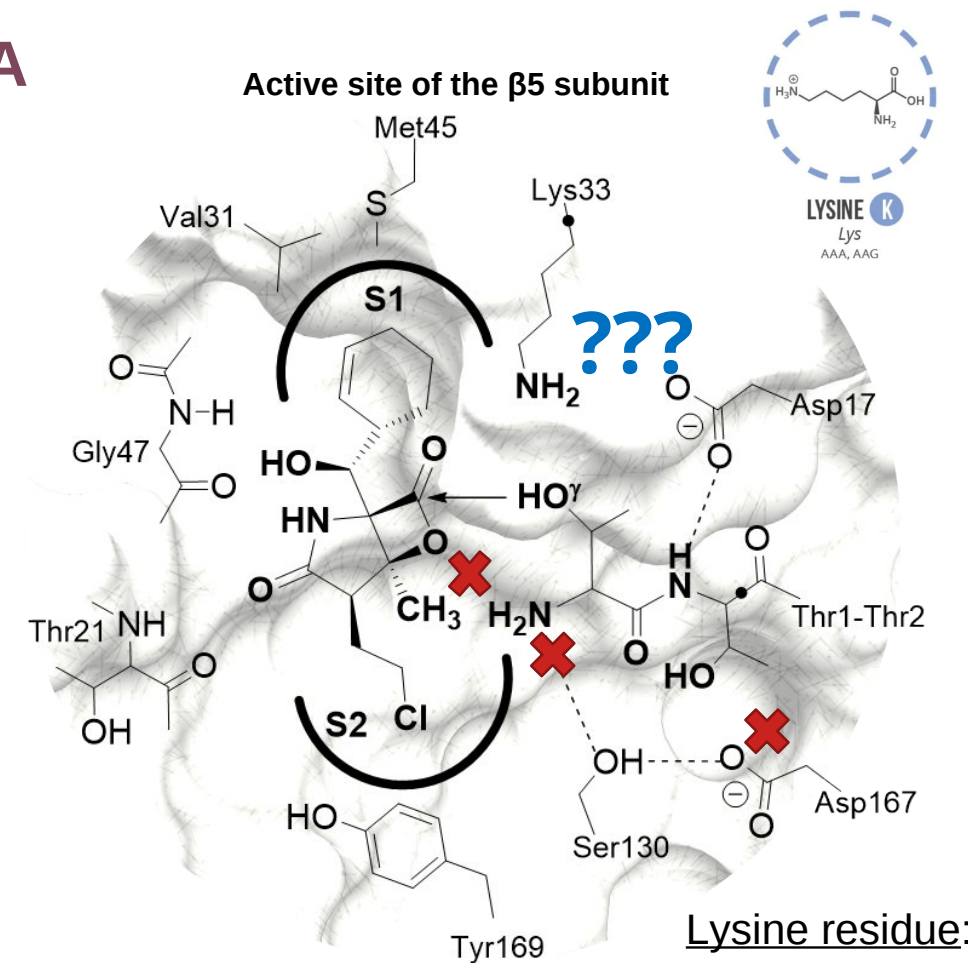
SalA-assisted mechanism



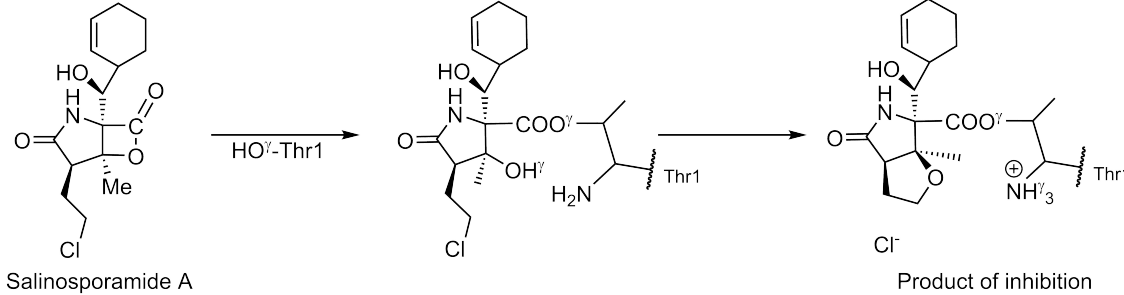
Huber E.M. et al. *Nat. Commun.* **2016**, 7, 10900
Groll, M. et al. *Marine Drugs* **2018**, 16, 240

Lys-assisted mechanism

Active site of the β_5 subunit

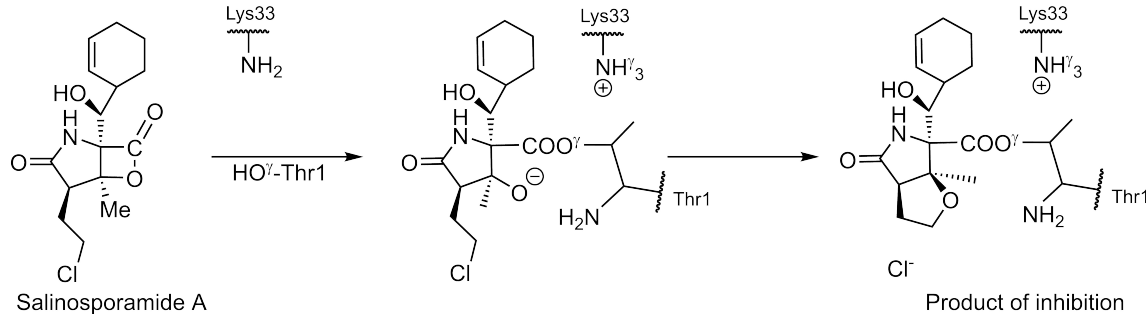


20S PROTEASOME INHIBITION WITH SalA



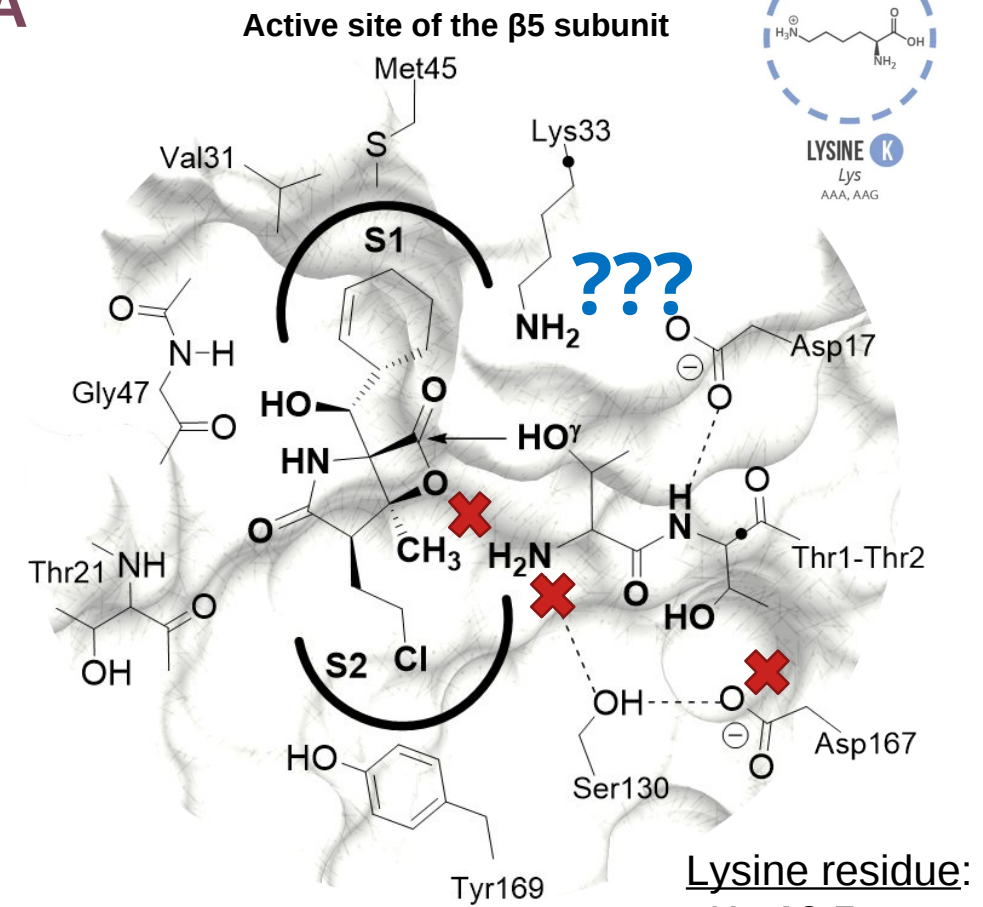
Groll, M. et al. *J. Am. Chem. Soc.* **2006**, 128, 5136-5141
Macherla, V.R. et al. *J. Med. Chem.* **2005**, 48, 3684-3687

SalA-assisted mechanism

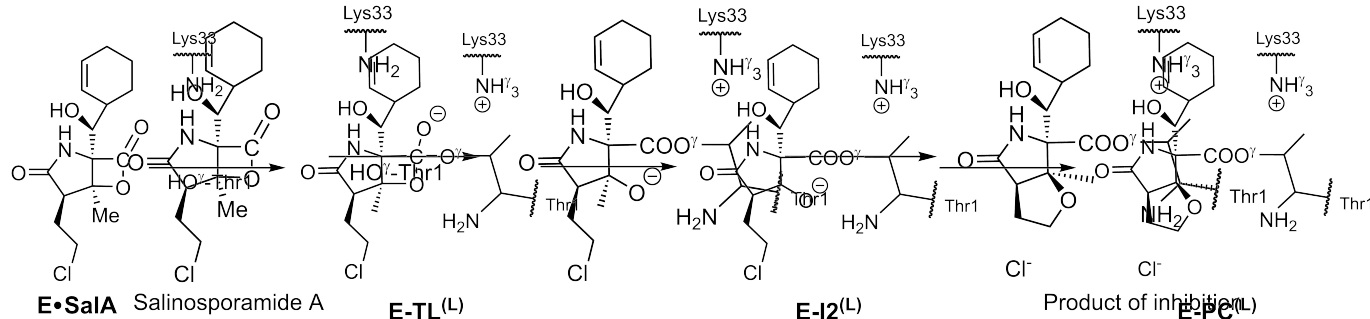


Huber E.M. et al. *Nat. Commun.* **2016**, 7, 10900
Groll, M. et al. *Marine Drugs* **2018**, 16, 240

Lys-assisted mechanism



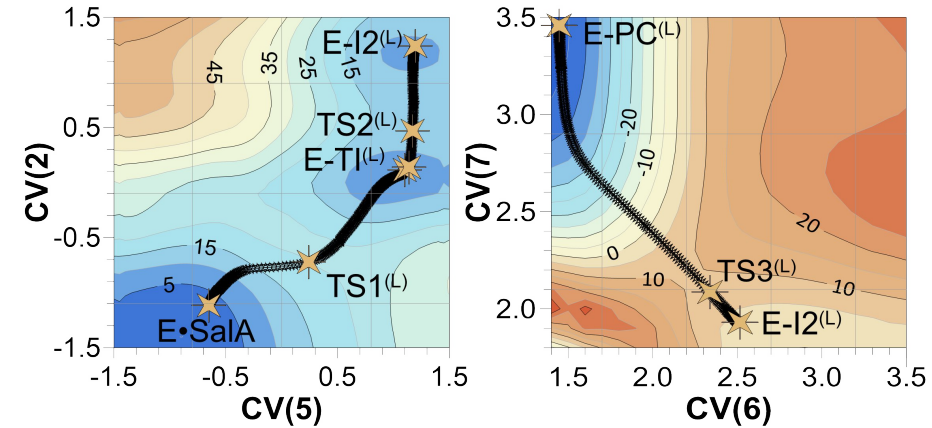
20S PROTEASOME INHIBITION WITH SalA



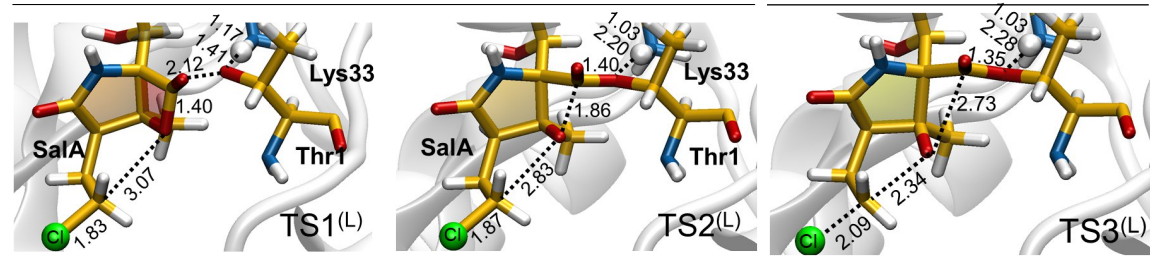
Herranz, F.M. et al. Nat. Commun. 2016, 7, 10202; 2021, 11, 3575–3589.
Groll, M. et al. *Marine Drugs* 2018, 16, 240

Lys-assisted mechanism

2D-PMF M06-2X:AM1/MM

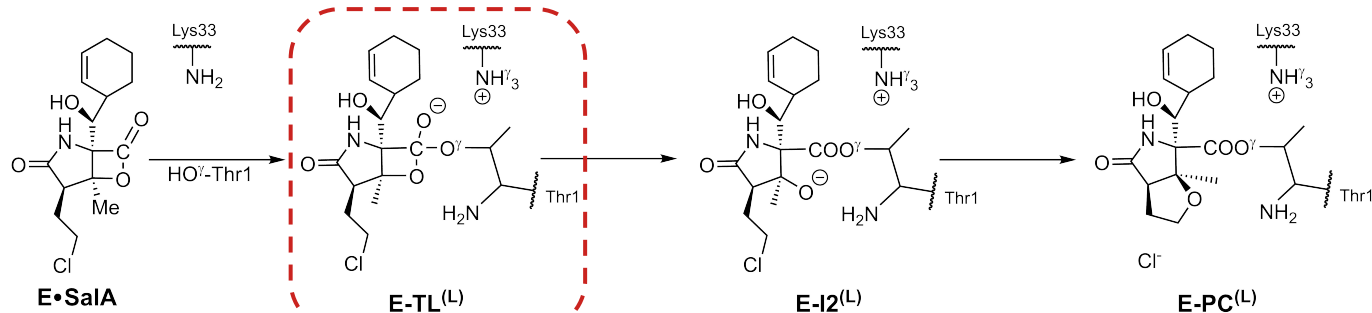


Applied collective variables are defined as follow:
 $CV(2) = d(O_2^{SalA}-C_1^{SalA}) - d(O^{yThr1}-C_1^{SalA})$, $CV(5) = d(O^{yThr1}-H^{yThr1}) - d(H^{yThr1}-N^{zLys33})$,
 $CV(6) = d(O_2^{SalA}-C_3^{SalA})$, and $CV(7) = d(C_3^{SalA}-Cl)$.



TS structures at M06-2X/MM

20S PROTEASOME INHIBITION WITH SalA



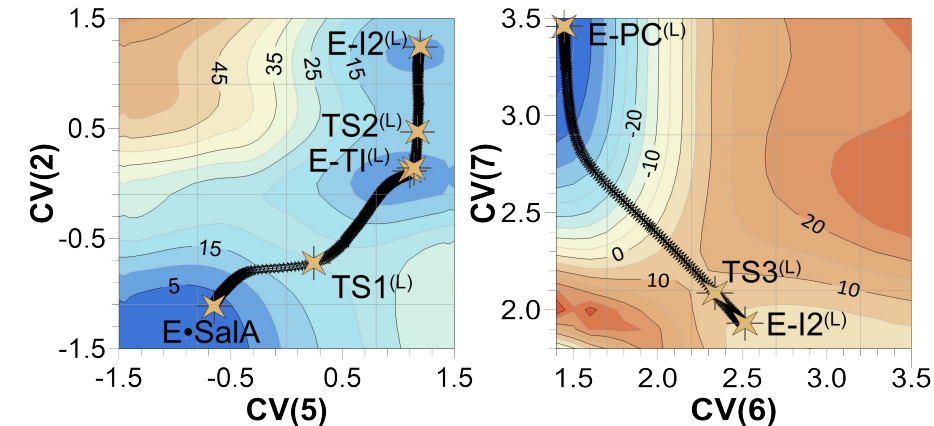
Serrano-Aparicio, N. et al. ACS Catal. 2021, 11, 3575–3589.

The existence of E-TI is especially interesting since the formation of a tetrahedral intermediate was previously excluded based on experimental studies on β -lactone inhibitors in **serine proteases**.

It was suggested that the tetrahedral TSs generated in the acylation reaction may **not be stabilized**, and thus the relief of high ring strain energy associated with the lactone ring cleavage may constitute the driving force for the acylation reaction.

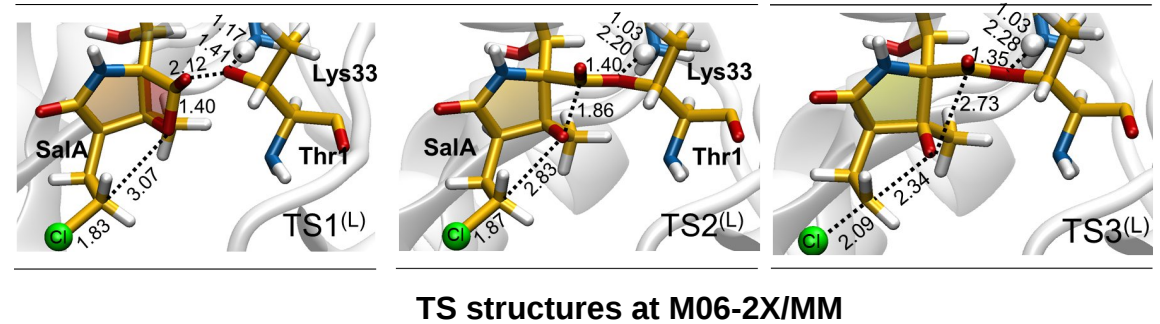
Kim, D. H. et al. Bioorganic Med. Chem. 2002, 10, 2553–2560

2D-PMF M06-2X:AM1/MM

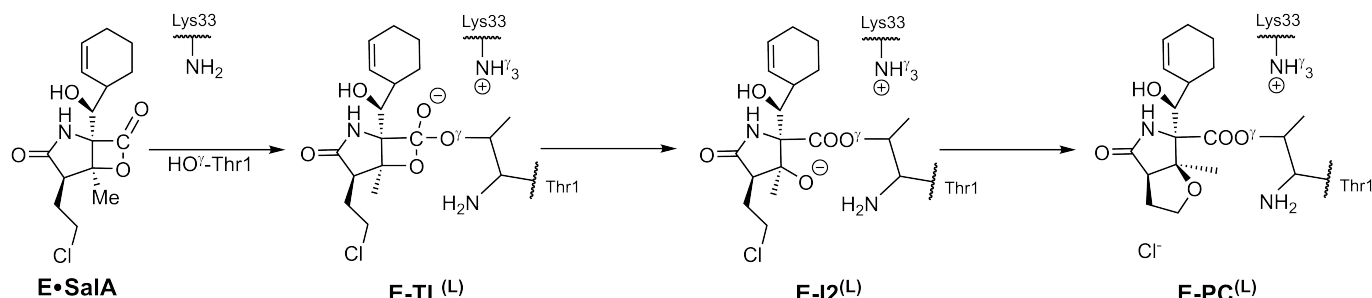


Applied collective variables are defined as follow:

$$\begin{aligned} \text{CV}(2) &= d(\text{O}^2\text{SalA}-\text{C}1\text{SalA}) - d(\text{O}^y\text{Thr1}-\text{C}1\text{SalA}), \text{CV}(5) = d(\text{O}^y\text{Thr1}-\text{H}^y\text{Thr1}) - d(\text{H}^y\text{Thr1}-\text{N}^z\text{Lys33}), \\ \text{CV}(6) &= d(\text{O}^2\text{SalA}-\text{C}3\text{SalA}), \text{and } \text{CV}(7) = d(\text{C}3\text{SalA}-\text{Cl}). \end{aligned}$$

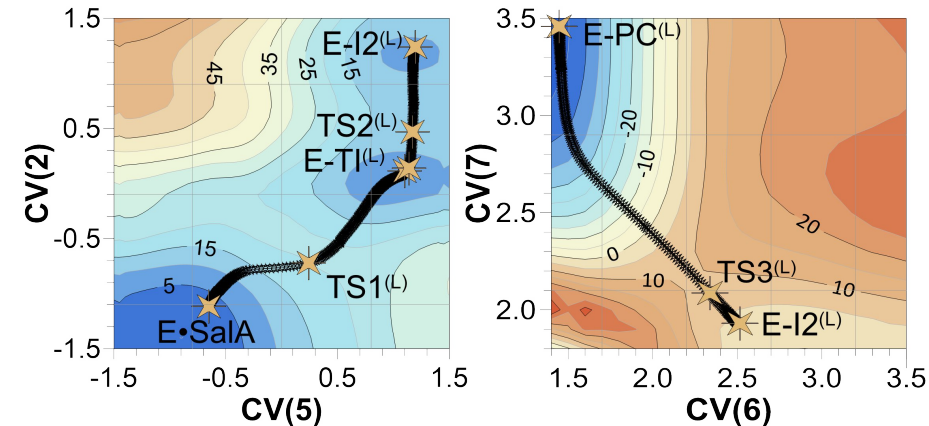


20S PROTEASOME INHIBITION WITH SalA

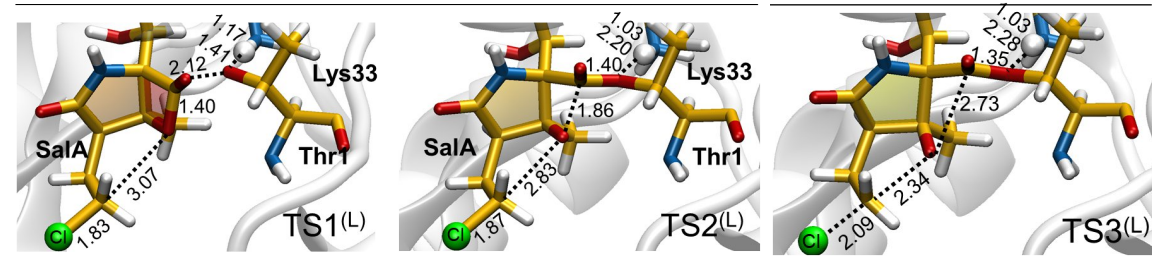
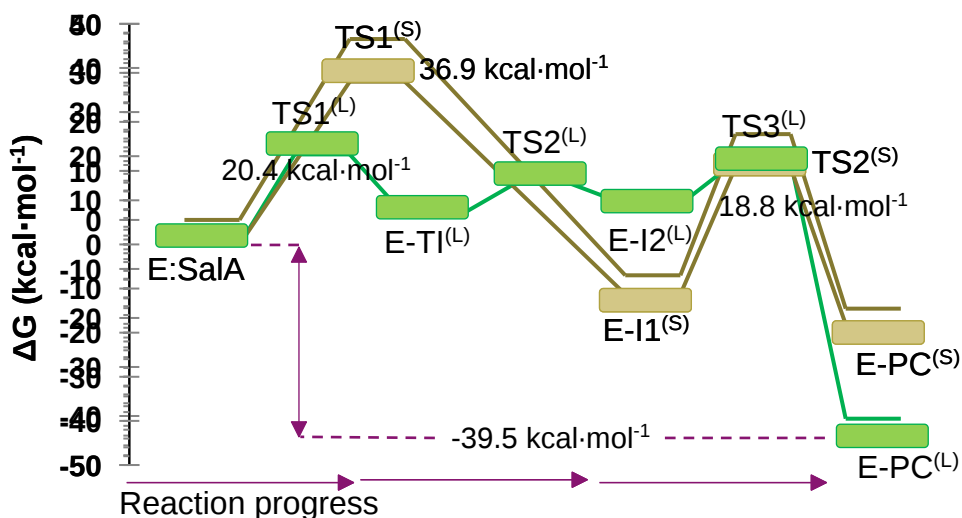


Serrano-Aparicio, N. et al. ACS Catal. 2021, 11, 3575–3589.

2D-PMF M06-2X:AM1/MM



Applied collective variables are defined as follow:
 $CV(2) = d(O_2^{SalA}-C_1^{SalA}) - d(O^{Y\text{Thr}1}-C_1^{SalA})$, $CV(5) = d(O^{Y\text{Thr}1}-H^{Y\text{Thr}1}) - d(H^{Y\text{Thr}1}-N^{\gamma\text{Lys}33})$,
 $CV(6) = d(O_2^{SalA}-C_3^{SalA})$, and $CV(7) = d(C_3^{SalA}-Cl)$.

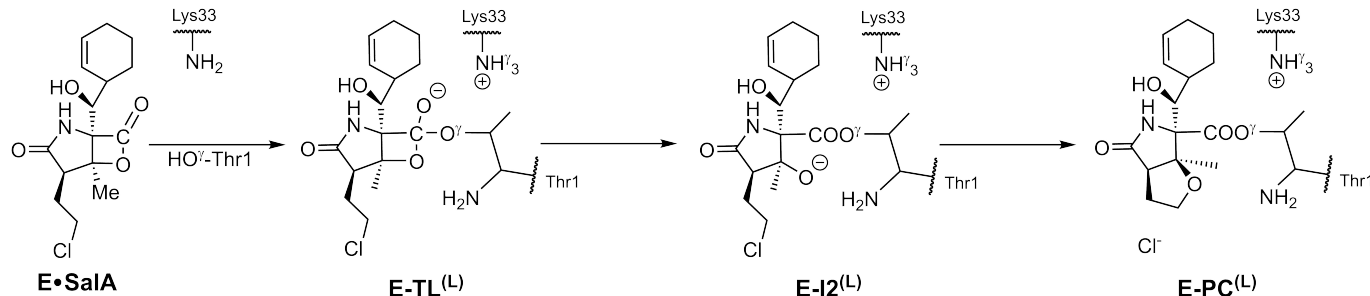


TS structures at M06-2X/MM

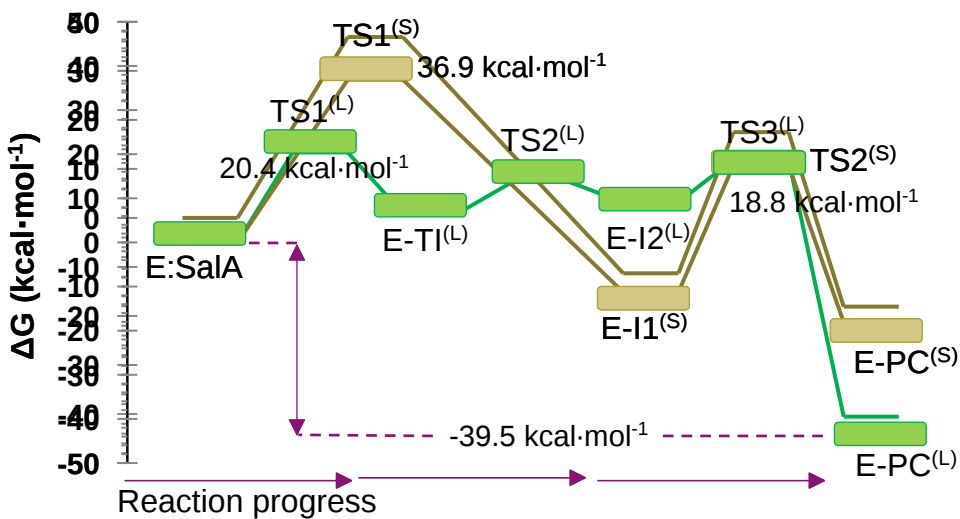
Exp. k_{inact} of 0.015 s^{-1}
 $(20.9\text{ kcal}\cdot\text{mol}^{-1}$ at $T=37\text{ }^\circ\text{C}$)

Manam, R. R et al. J. Med. Chem. 2008, 51, 6711–6724.

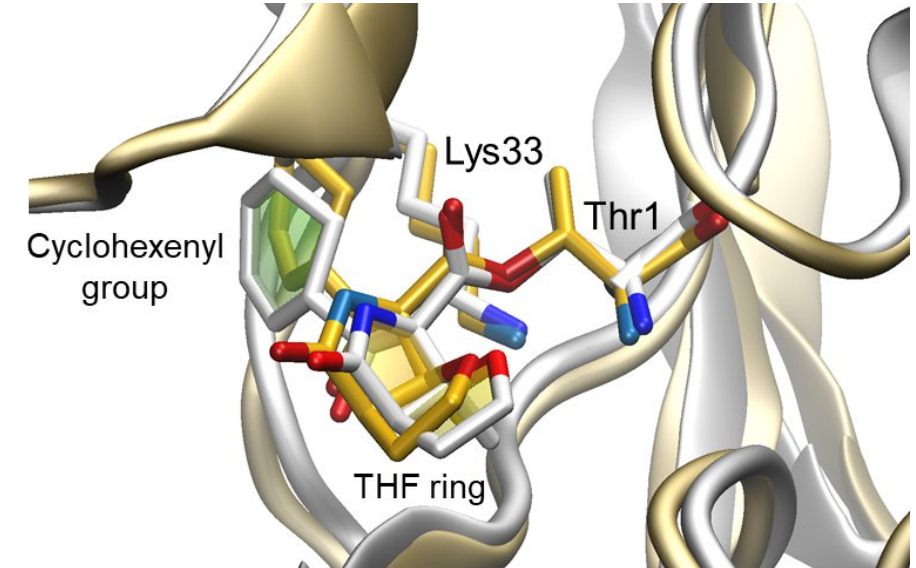
20S PROTEASOME INHIBITION WITH SalA



Serrano-Aparicio, N. et al. ACS Catal. 2021, 11, 3575–3589.

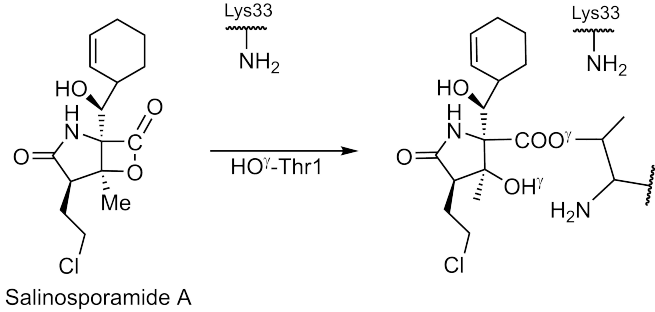


*Exp. k_{inact} of 0.015 s⁻¹
(20.9 kcal·mol⁻¹ at T= 37 °C)*

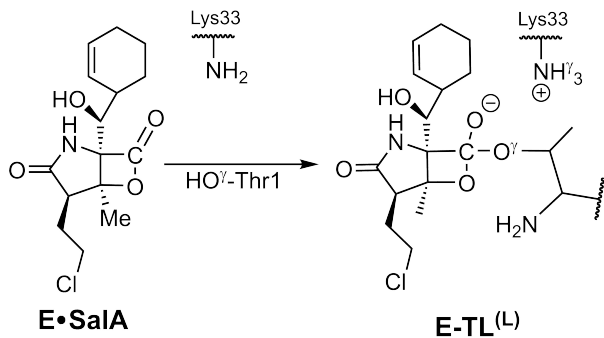


Overlay of the crystal structure of 20S proteasome in complex with SalA with PDB code 2FAK, (in grey) and the product complex obtained from our QM/MM MD studies of the Lys33-assisted reaction pathway (in orange).

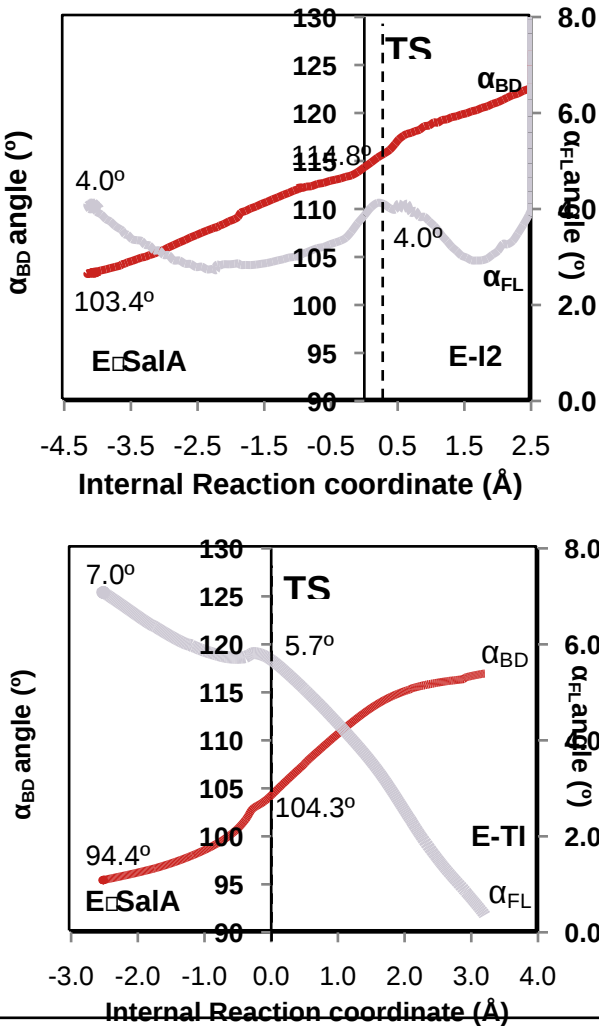
20S PROTEASOME INHIBITION WITH SalA



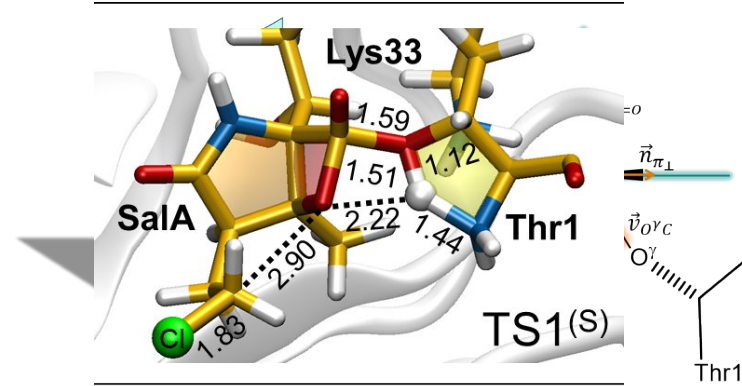
Groll, M. et al. *J. Am. Chem. Soc.* **2006**, 128, 5136–5141
Macherla, V.R. et al. *J. Med. Chem.* **2005**, 48, 3684–3687



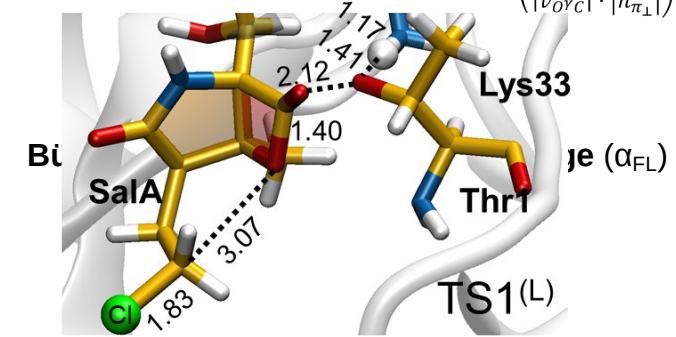
Serrano-Aparicio, N. et al. *ACS Catal.* **2021**, 11, 3575–3589.



Nucleophilic attack trajectory



$$\alpha_{BD} = \pi - (\text{Nu:}-C=O) \quad \alpha_{FL} = \arcsin \left(\frac{|\vec{v}_{O\gamma C} \cdot \vec{n}_{\pi\perp}|}{|\vec{v}_{O\gamma C}| \cdot |\vec{n}_{\pi\perp}|} \right)$$

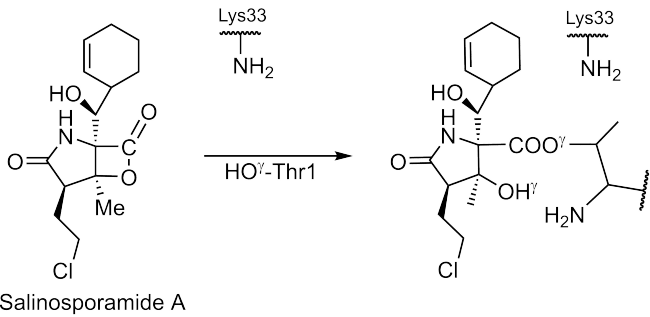


Bürgi, H. B. et al. *J. Am. Chem. Soc.* **1973**, 95, 5065–5067.

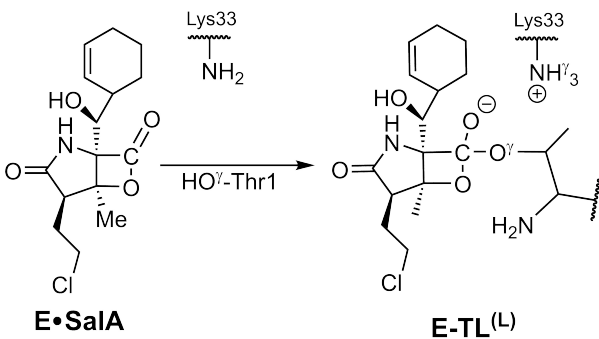
Bürgi, H. B. et al. *Tetrahedron* **1974**, 30, 1563–1572.

Heathcock, C.H. *Aldrichimica Acta*, **1990**, 23, 94–111.

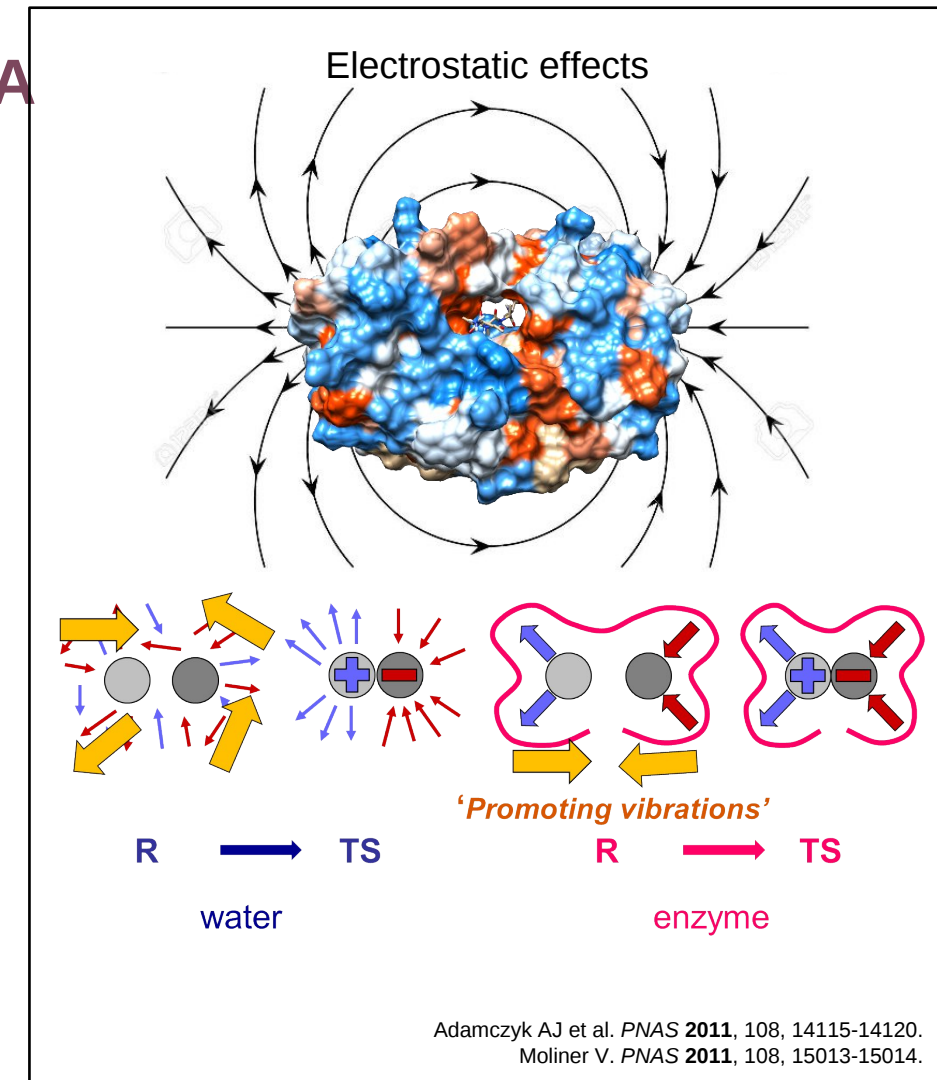
20S PROTEASOME INHIBITION WITH SalA

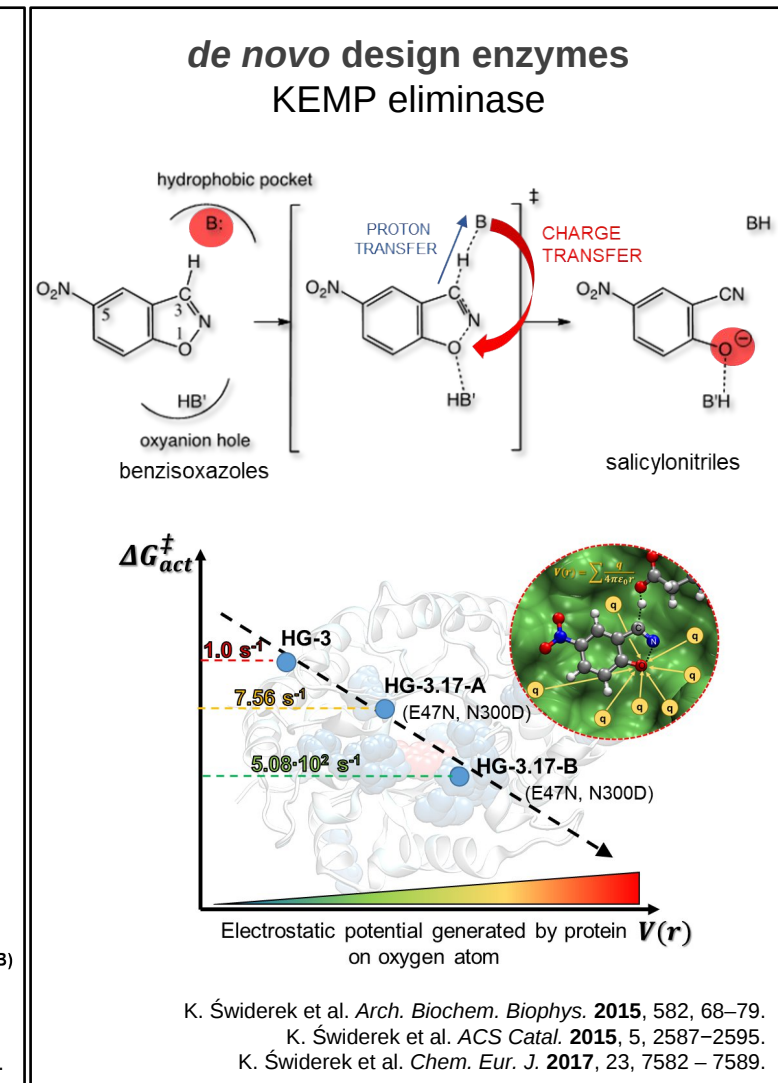
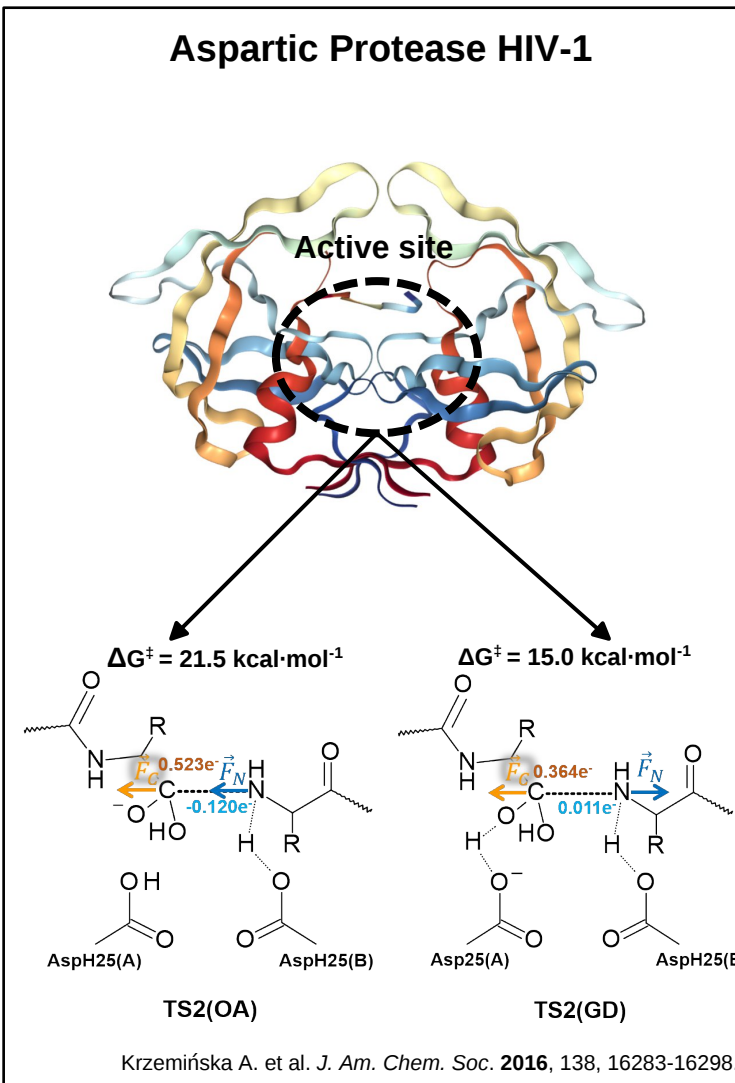
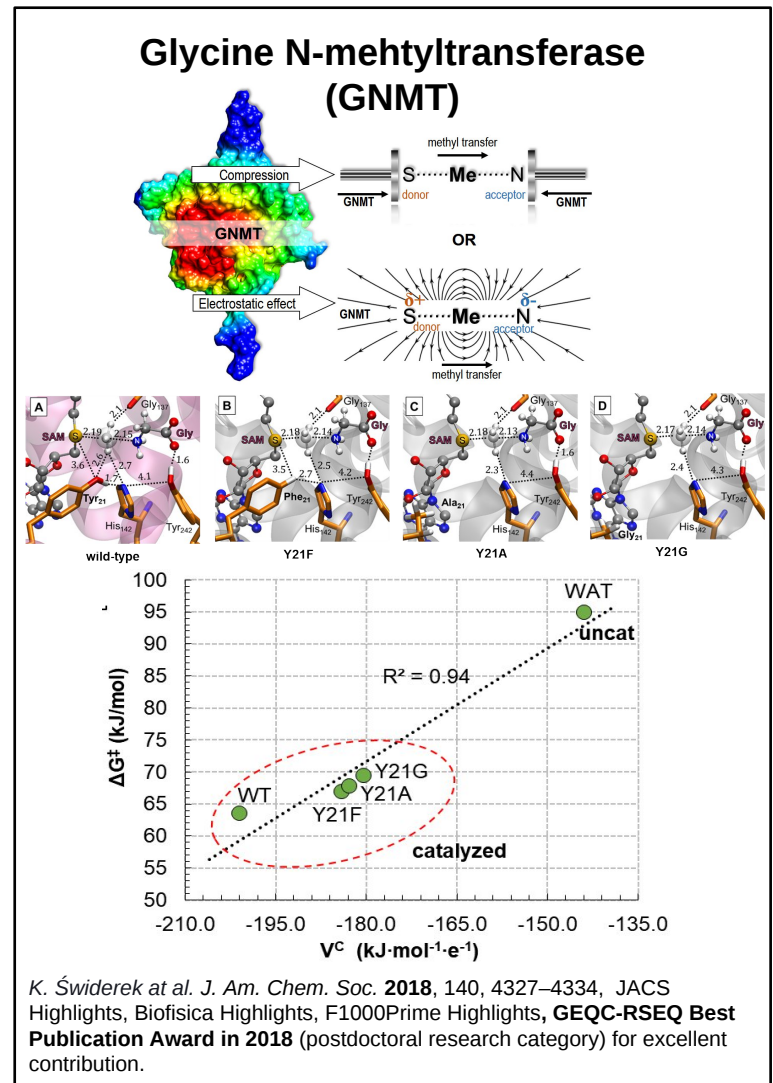


Groll, M. et al. *J. Am. Chem. Soc.* **2006**, 128, 5136–5141
 Macherla, V.R. et al. *J. Med. Chem.* **2005**, 48, 3684–3687

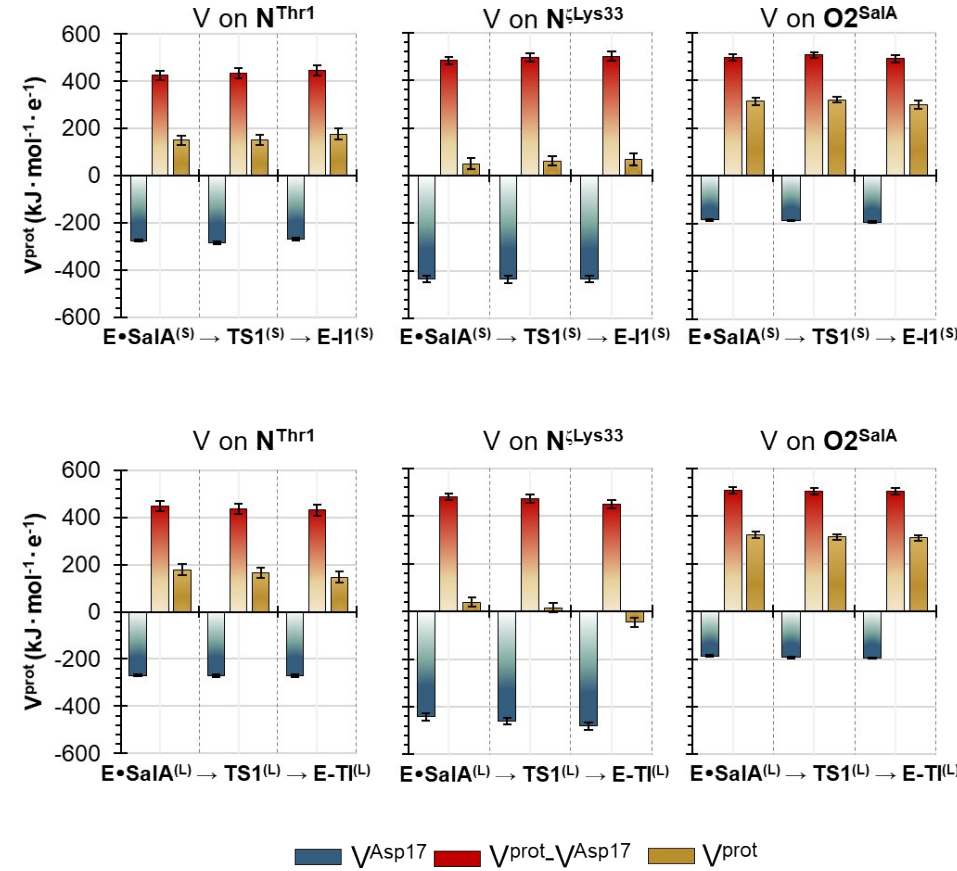
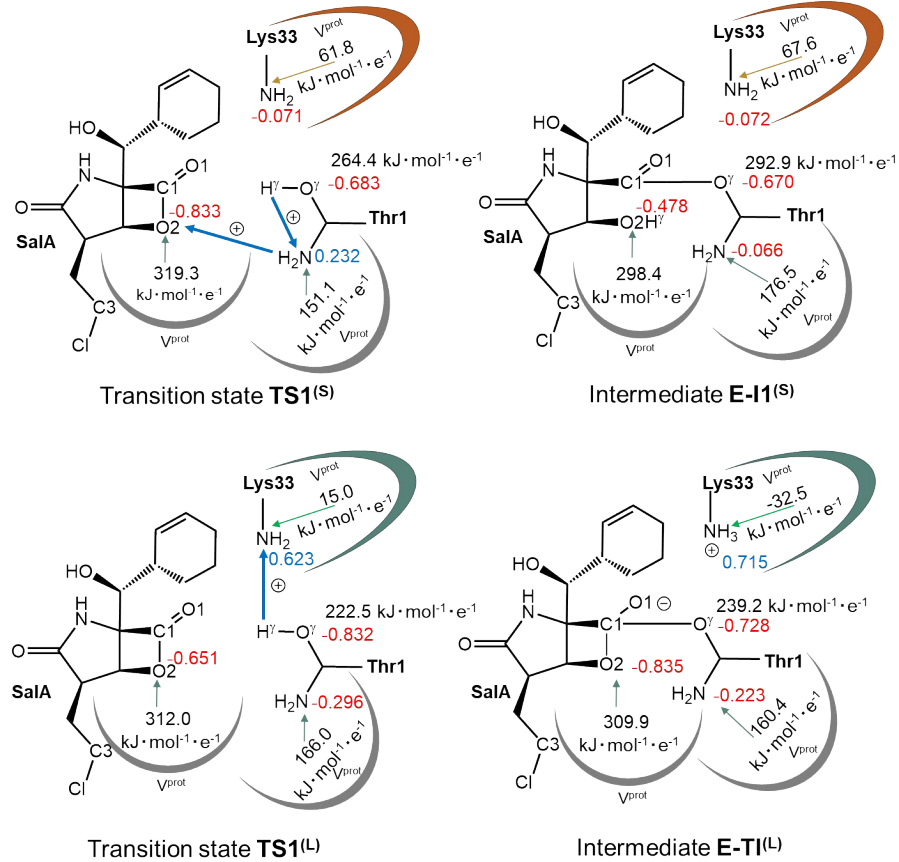


Serrano-Aparicio, N. et al. *ACS Catal.* **2021**, 11, 3575–3589.

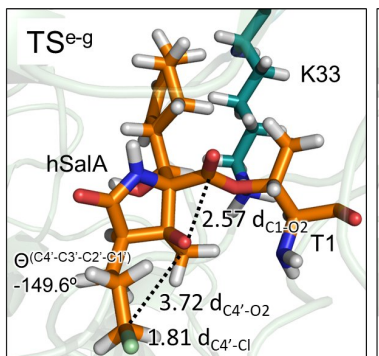
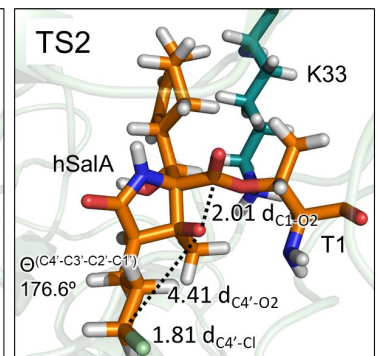
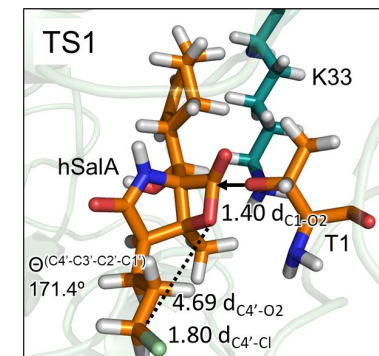
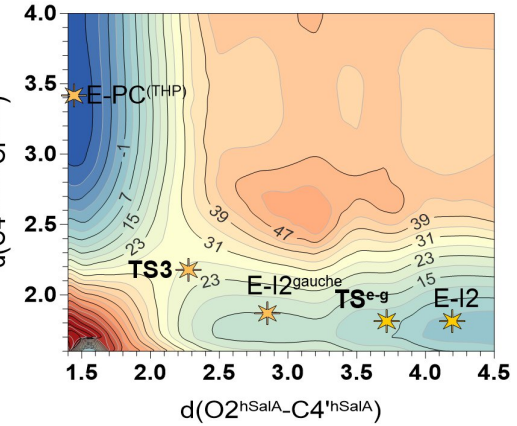
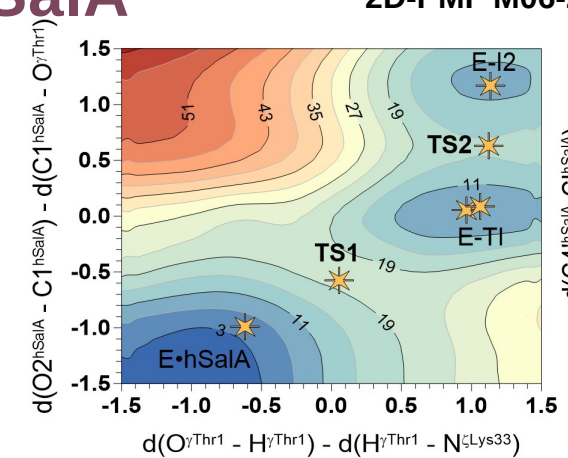
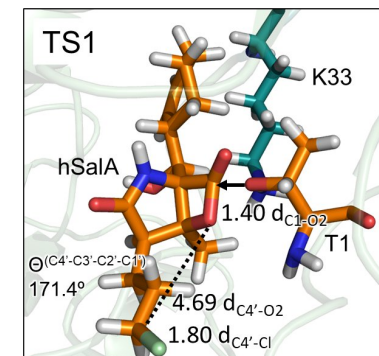
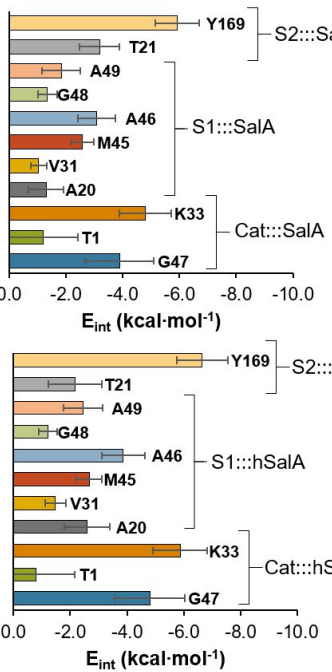
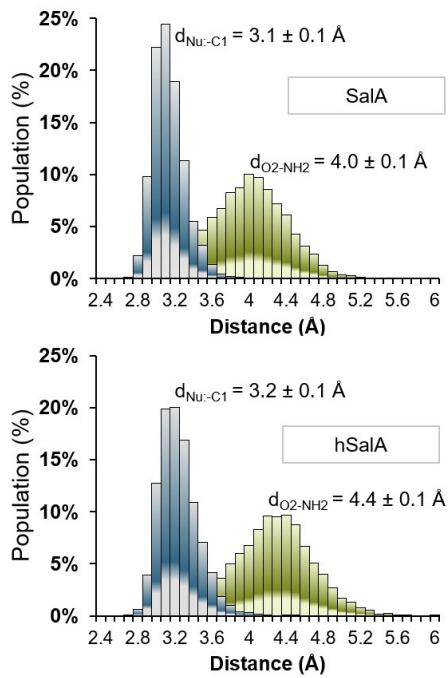
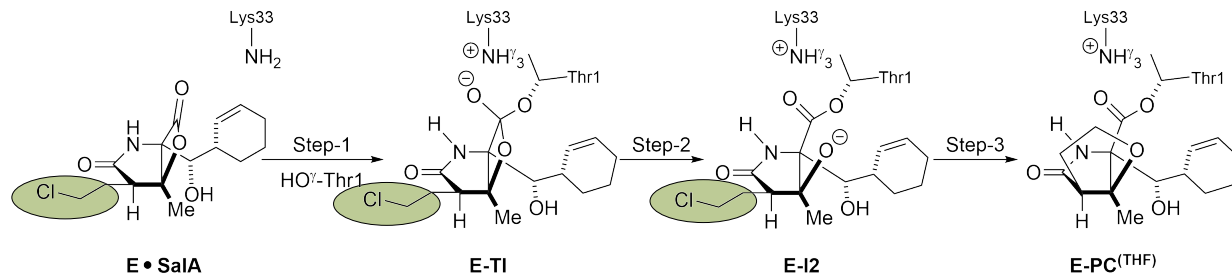




20S PROTEASOME INHIBITION WITH SalA

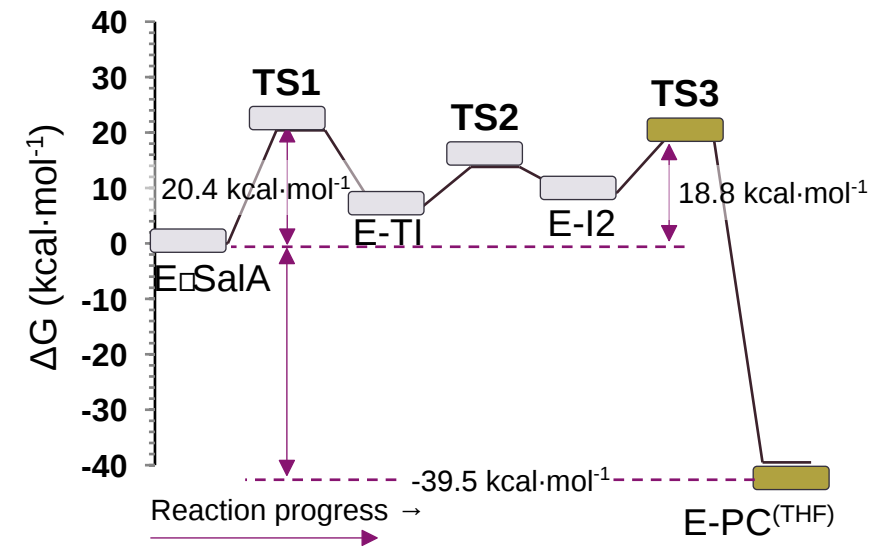
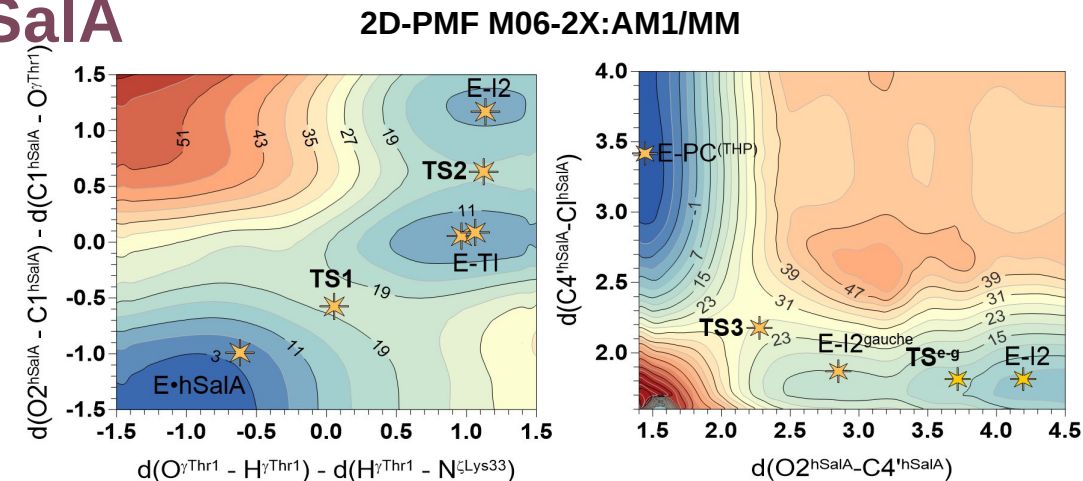
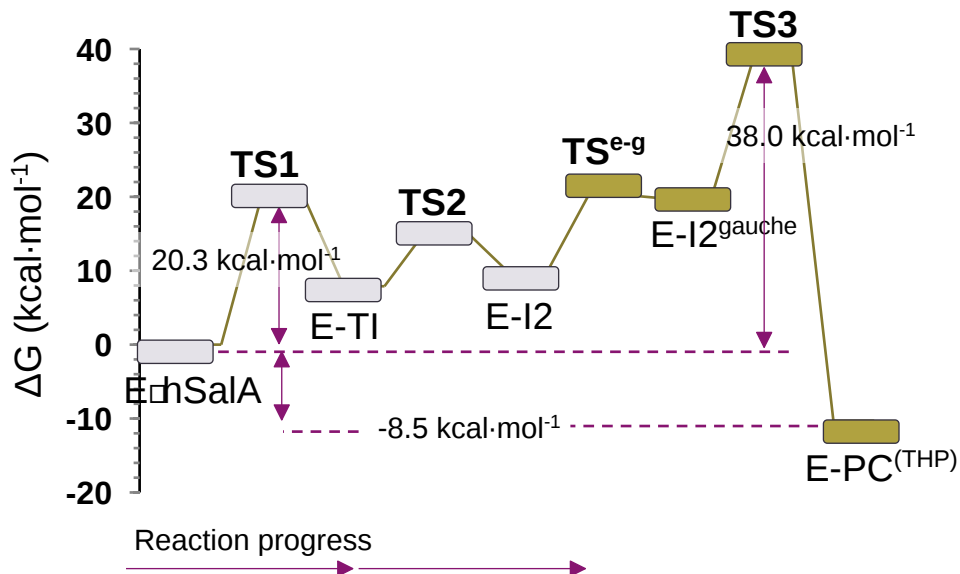
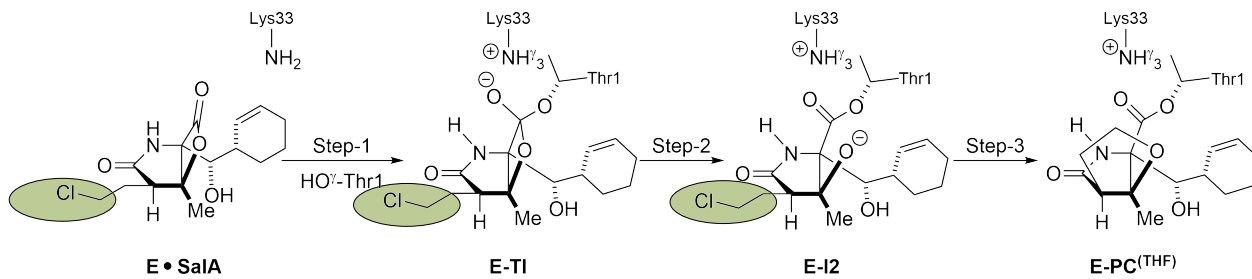


20S PROTEASOME INHIBITION WITH hSalA

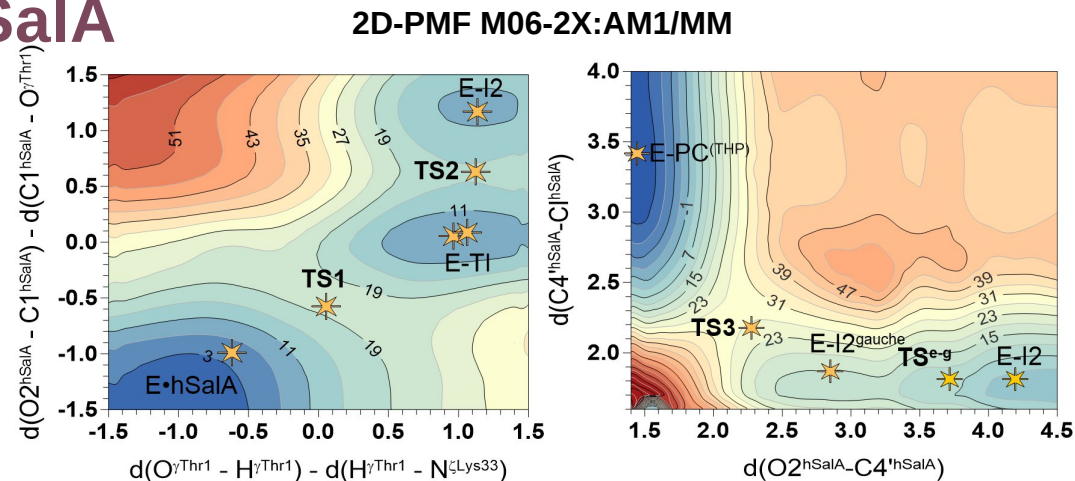
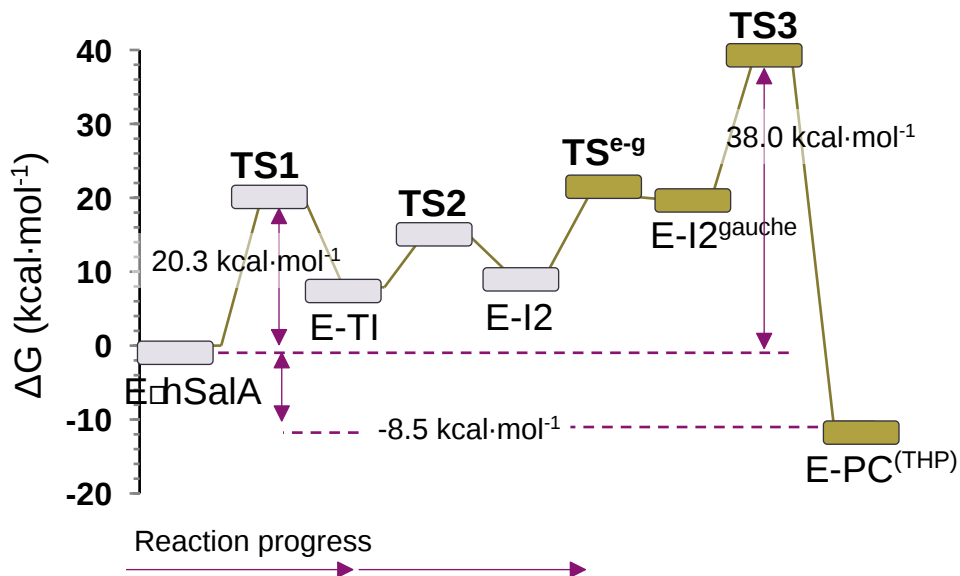
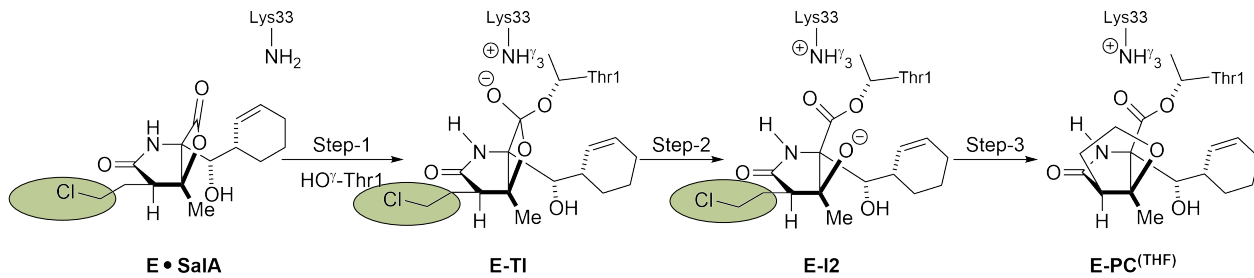


TS structures at M06-2X/MM

20S PROTEASOME INHIBITION WITH hSalA



20S PROTEASOME INHIBITION WITH hSalA



- (i) how is it possible that the final **E-I2 product complex** that corresponds to the one observed in the crystal structure is not thermodynamically stable as deduces from free energy surfaces?;
- (ii) is the reversible character of the hSalA inhibitor controlled by **reversible dissociation** of the inhibitor from the active site or is it dictated by an additional step involving **slow hydrolysis of the ester linkage**?

FORMATION OF THP vs. THF

The proposed hypothesis explaining the absence of the THP in the crystal structure suggests that a **longer chloro-n-propyl** group of hSalA **adopts an extended conformation** in the active site of proteasome that **can prevent the ring closure**.

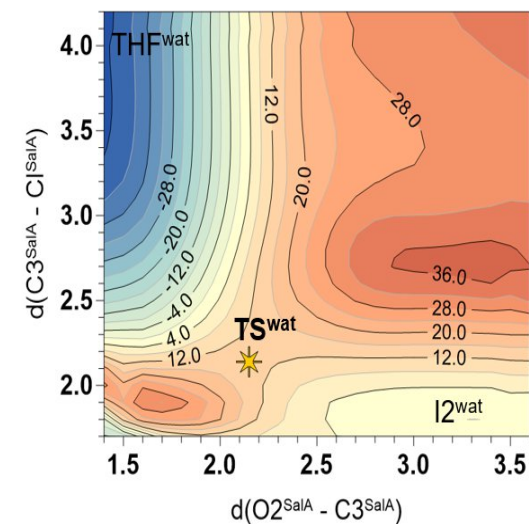
However, in the same studies, it was shown that this group is highly flexible, which was confirmed by **experimentally measured high values of B-factor** for this fragment. Therefore, it is expected that **rotation from extended to closed conformer should not be expensive**.

It was found that the gauche conformer is metastable intermediate in the enzyme, which confirms the prediction from experimental studies that assumes a **short half-time** for this inhibitor sidechain orientation.

Free energy computed for THF and THP formation (PC) in the aqueous solution and the active site of the 20S proteasome. Values are given in $\text{kcal}\cdot\text{mol}^{-1}$.

	SalA		hSalA	
	water	enzyme	water	enzyme
E-I2 ^{extended}	-	-	-5.2	-9.7
E-I2/E-I2 ^{gauche}	0.0	0.0	0.0	0.0
TS	13.1	9.7	16.8	18.3
PC	-45.3	-48.6	-37.2	-30.0

A.



B.

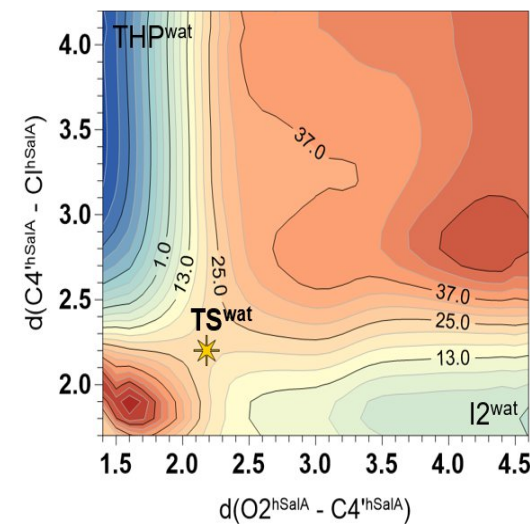
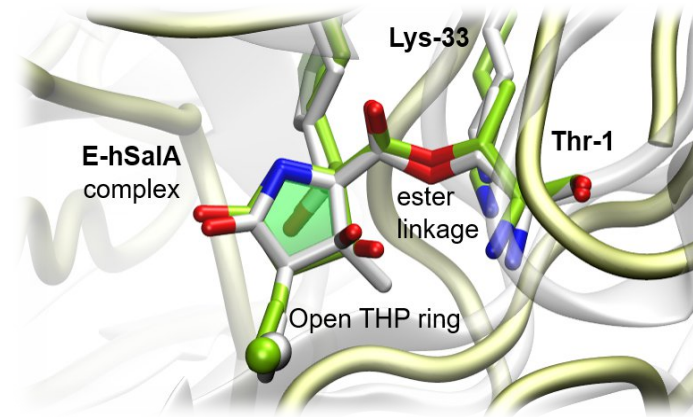
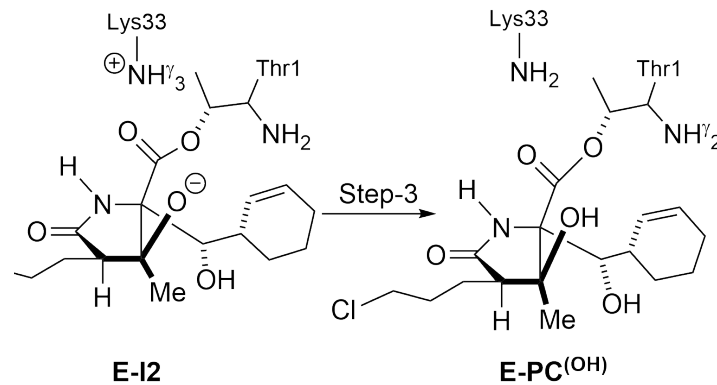


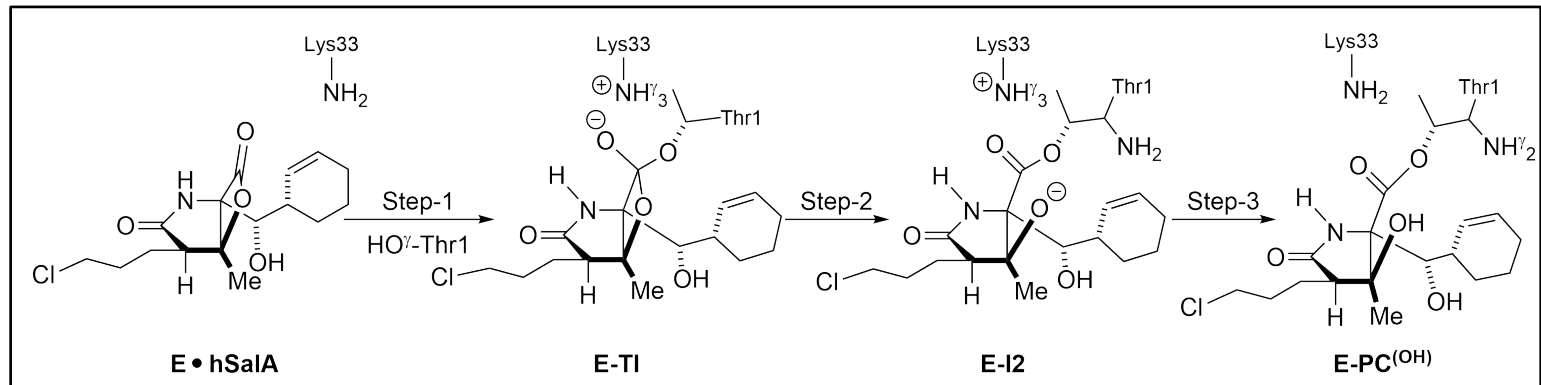
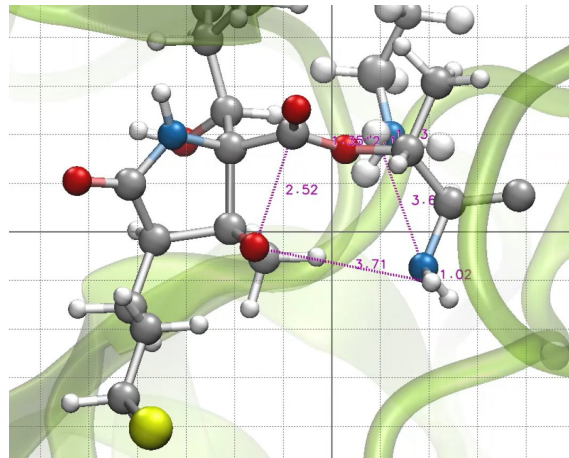
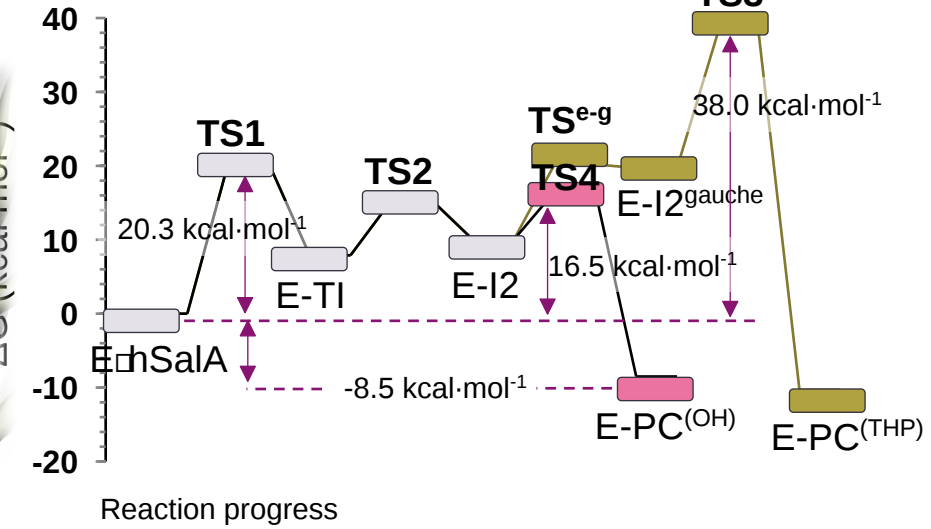
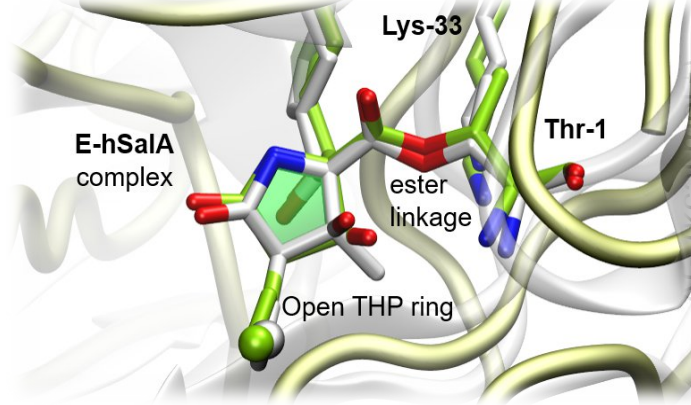
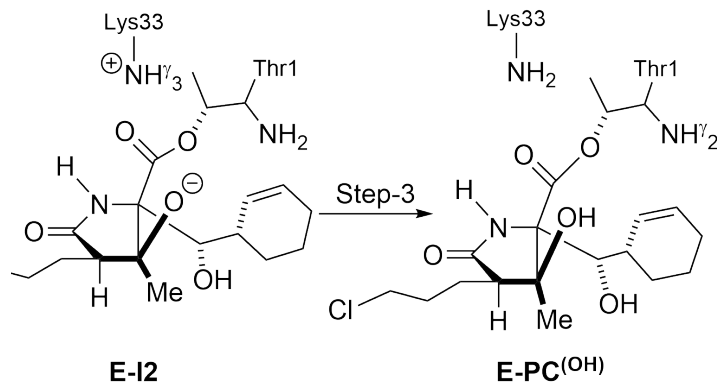
Figure 4. Free energy surfaces for intramolecular cyclization step for **A.** SalA and **B.** hSalA in the aqueous solution.

STABILIZATION OF THE FINAL INHIBITION PRODUCT



Overlay of the crystal structure of the final product of inhibition of β 5-subunit of yeast 20S proteasome (in grey) by hSalA with and human variant delivered from the M06-2X/MM optimization **E-PC^(OH)** (in green).

STABILIZATION OF THE FINAL INHIBITION PRODUCT



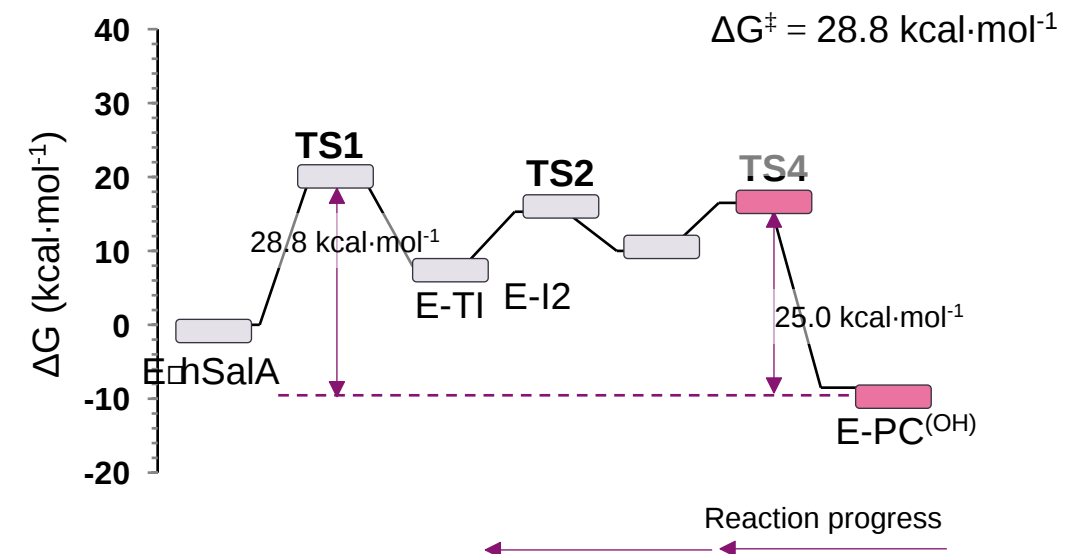
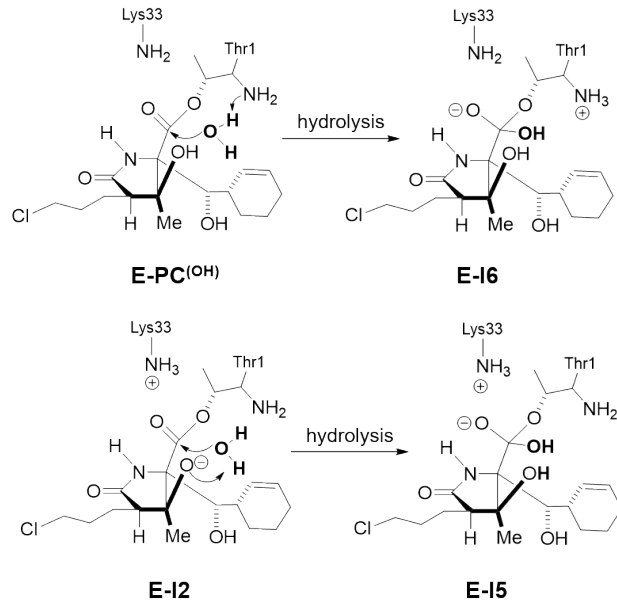
Overlay of the crystal structure of the final product of inhibition of β_5 -subunit of yeast 20S proteasome (in grey) by hSalA with and human variant delivered from the M06-2X/MM optimization E-PC(OH) (in green).

hSalA as COVALENT REVERSIBLE INHIBITOR

Table 1. Covalent inhibition strategy for SalA and hSalA.

	Class of inhibitor	Scheme ^[a]
Irreversible inhibition	Classical	$E + I \xrightleftharpoons{K_i} E \square I \xrightarrow{k_{inact}} E - I$
	Covalent reversible	$E + I \xrightleftharpoons{K_i} E \square I \rightleftharpoons E - I$
Reversible inhibition	Slow Substrate	$E + I \xrightleftharpoons{K_i} E \square I \longrightarrow E - I \longrightarrow E + P$ <i>slow</i>

[a] where the K_i is the inhibition constant that measures binding affinity, and k_{inact} is the inactivation rate constant, that measures chemical reactivity.

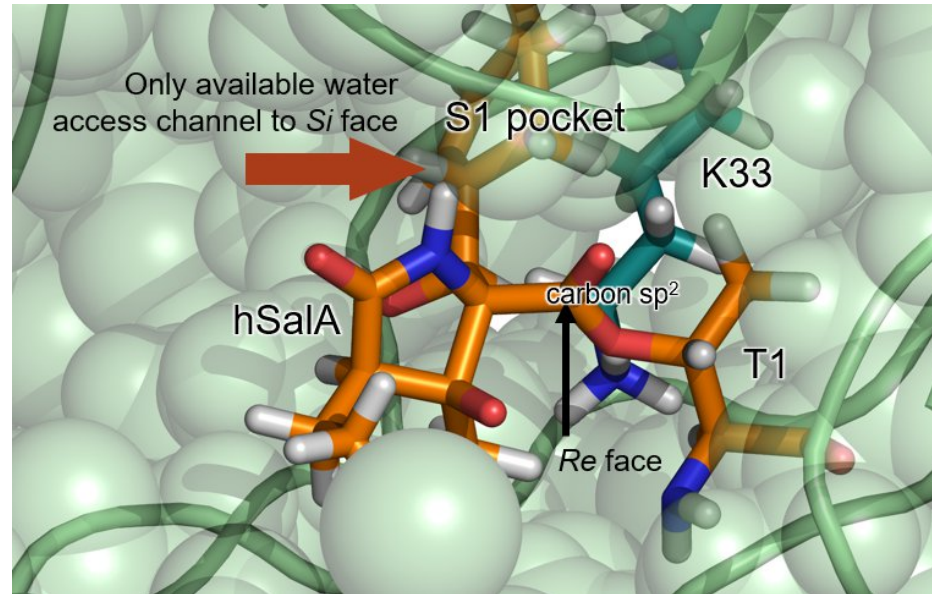
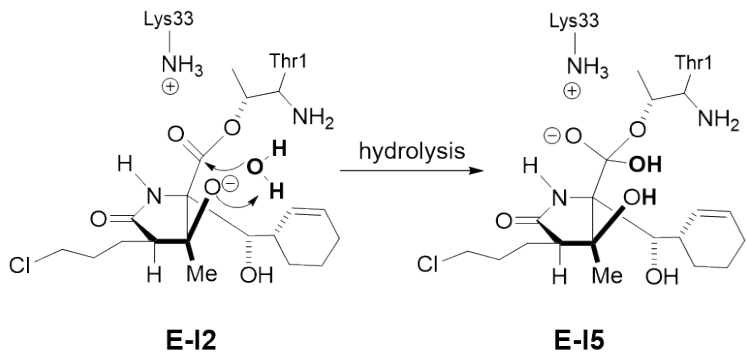
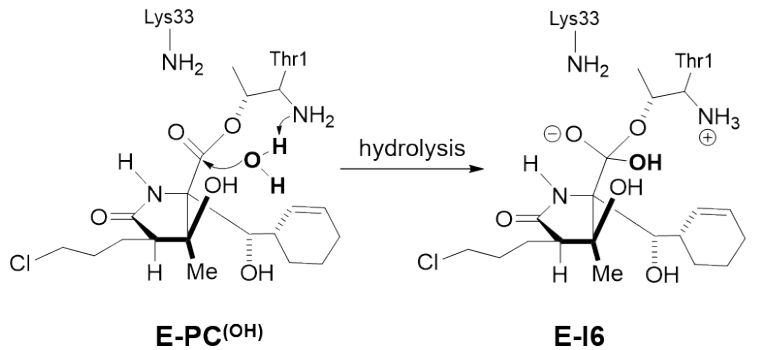


hSalA SLOW SUBSTRATE

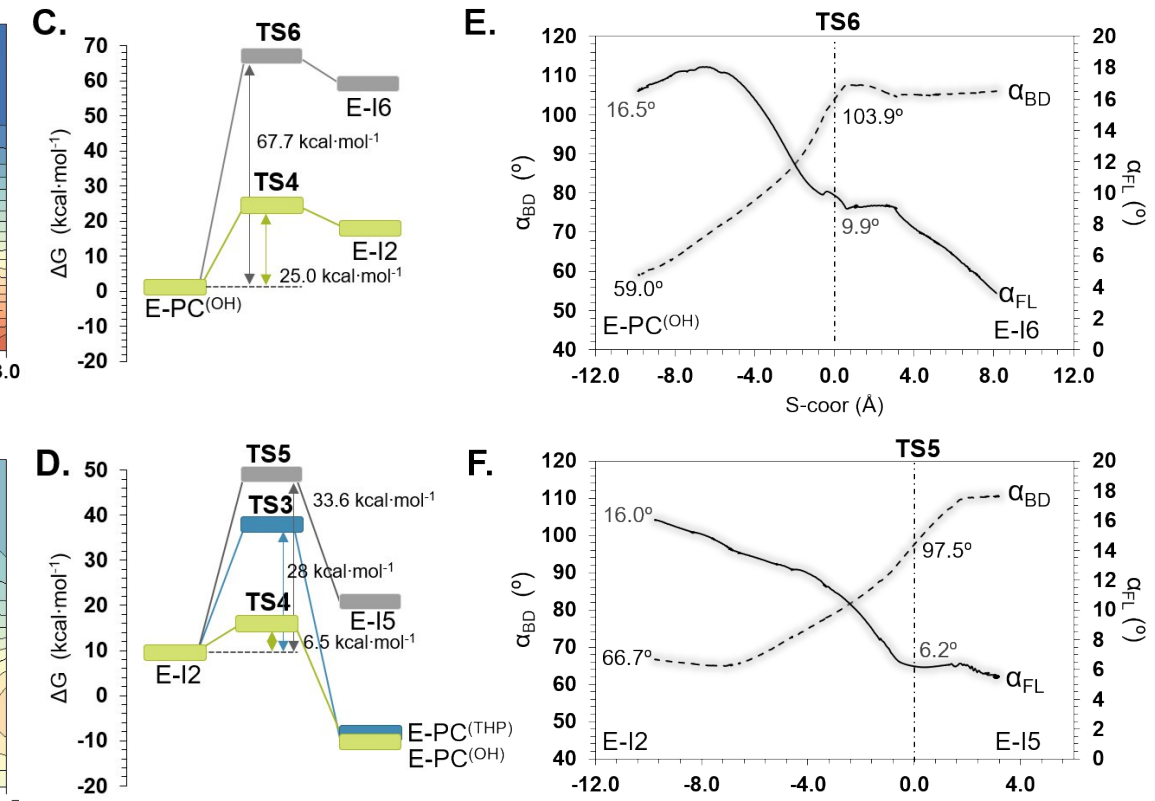
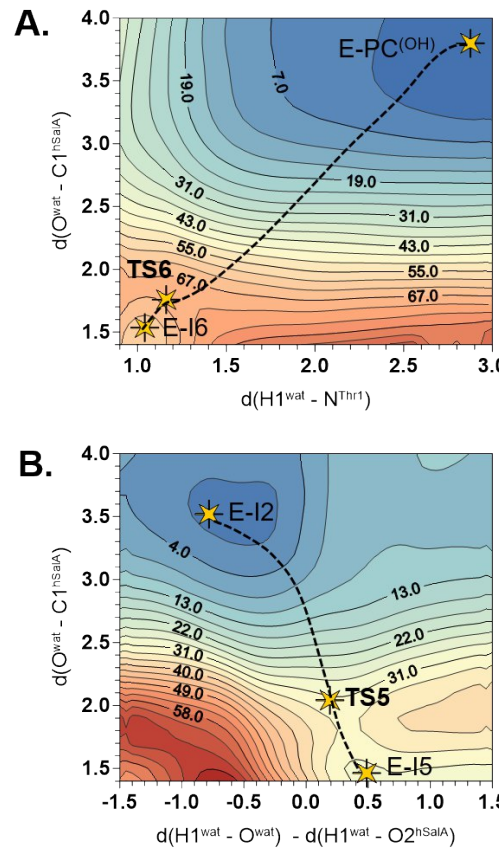
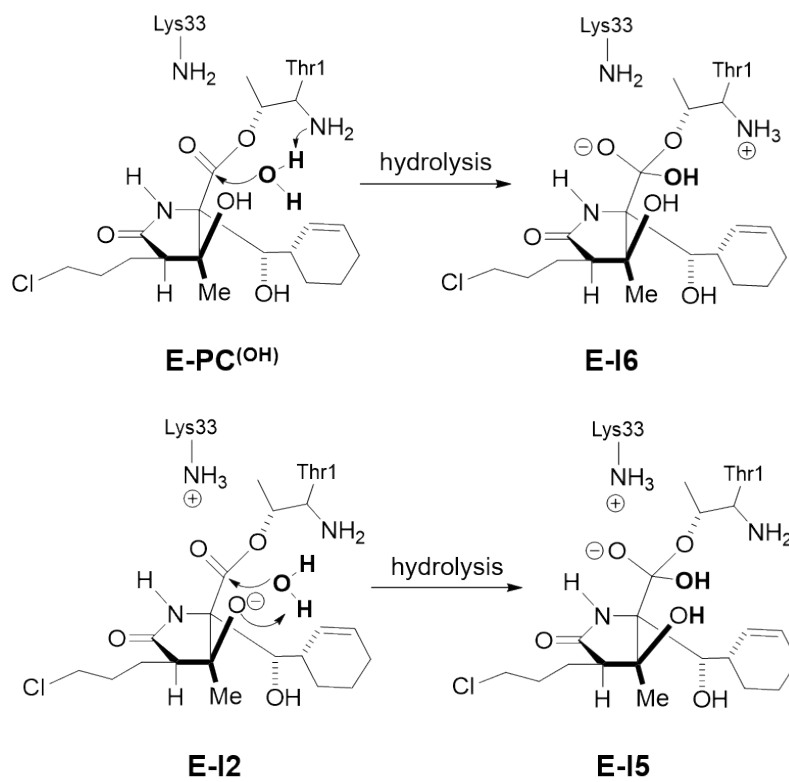
Table 1. Covalent inhibition strategy for SalA and hSalA.

	Class of inhibitor	Scheme ^[a]
Irreversible inhibition	Classical	$E + I \xrightleftharpoons{K_i} E \square I \xrightarrow{k_{inact}} E - I$
	Covalent reversible	$E + I \xrightleftharpoons{K_i} E \square I \rightleftharpoons E - I$
Reversible inhibition	Slow Substrate	$E + I \xrightleftharpoons{K_i} E \square I \longrightarrow E - I \longrightarrow E + P$ <i>slow</i>

[a] where the K_i is the inhibition constant that measures binding affinity, and k_{inact} is the inactivation rate constant, that measures chemical reactivity.



hSalA as a SLOW SUBSTRATE





Nature of Irreversible Inhibition of Human 20S Proteasome by Salinosporamide A. The Critical Role of Lys–Asp Dyad Revealed from Electrostatic Effects Analysis

Natalia Serrano-Aparicio, Vicent Moliner,* and Katarzyna Świderek*

Cite this: *ACS Catal.* 2021, 11, 6, 3575–3589

Publication Date: March 5, 2021 ▾

<https://doi.org/10.1021/acscatal.0c05313>

Copyright © 2021 The Authors. Published by American Chemical Society

[RIGHTS & PERMISSIONS](#)



On the Origin of the Different Reversible Characters of Salinosporamide A and Homosalinosporamide A in the Covalent Inhibition of the Human 20S Proteasome

Natalia Serrano-Aparicio, Vicent Moliner,* and Katarzyna Świderek*

Cite this: *ACS Catal.* 2021, 11, 18, 11806–11819

Publication Date: September 8, 2021 ▾

<https://doi.org/10.1021/acscatal.1c02614>

Copyright © 2021 The Authors. Published by American Chemical Society

[RIGHTS & PERMISSIONS](#)

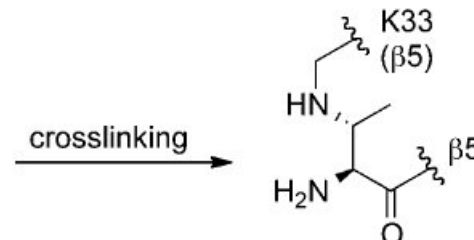
Cover of Issue 6, 2021
ACS Catal., 2021, **11**, 3575–3589

SUMMARY

- A new mechanism of inhibition with **SalA** was proposed, that involved the active role of the Lys33-Asp17 diad in the active site of Proteasome 20S.
- **Intramolecular Cyclization Step** Determines the Character of the Human 20S Proteasome Covalent Inhibition with SalA and hSalA.

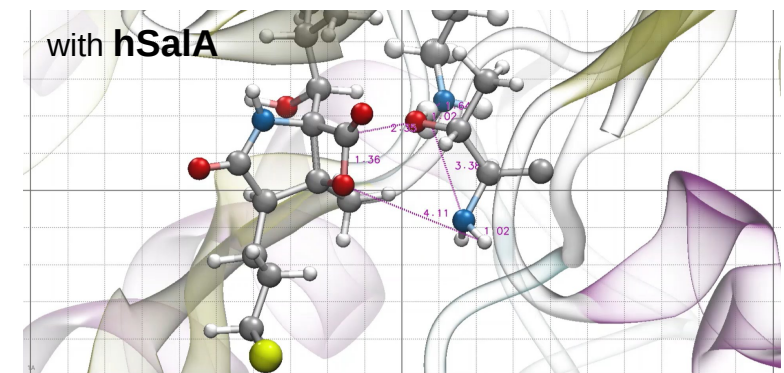
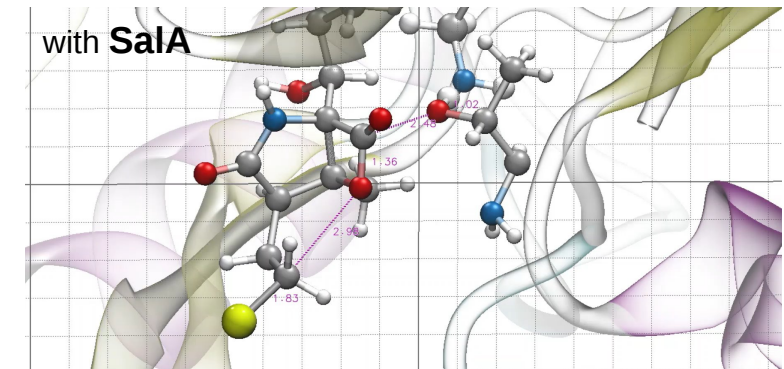
PERSPECTIVES

- Is role of Lys33-Asp17 confirmed for **autolysis and proteolysis** processes?
- How is **K33A variant** still able to catalyze this process with reduced activity?
- A novel reaction mechanism involving irreversible crosslinking of the proteasomal active site (**K33-T1 crosslink**)



- Designing of new inhibitors in collaboration with Dr F. González (UJI, Spain) and Prof. A. Chari (Max Planck Institut, Germany)

Mechanism of Covalent Inhibition of β 5-subunit of 20S Proteasome



MEPs computed at M06-2X/MM level

ACKNOWLEDGEMENTS

StopProt Research Team:

Natalia Serrano Aparicio, PhD candidate (Universtat Jaume I, Spain)

Miquel Àngel Galmés, PhD candidate (Universtat Jaume I, Spain)

Silvia Ferrer, Personal técnico de apoyo, PhD candidate (Universtat Jaume I, Spain)

Vicent Moliner, Prof. (Universitat Jaume I, Spain)

Alessio Lodola, Dr. (University of Parma, Italy)

Florenci González, Dr. ((Universtat Jaume I, Spain)

Carmen Domene, Prof.(University of Bath, UK)

Recent fundings and resources:



Ramon y Cajal contract and JIN project
(RYC2020-030596-I and PID2019-107098RJ-I00)
Ministerio de Ciencia, Innovación y Universidades,
2020



(UJI-A2019-04)
Universitat Jaume I, 2019



**GENERALITAT
VALENCIANA**

(SEJI/2020/007)

Subvenciones Excelencia Científica Juniors Investigadores,
GVA, GenT-SEJI 2020

T·R·I·N·I·T·Y cluster: 320 CPUs and 10 Geforce RTX 3090 Turbo 24GB GDDR6X funded by GVA-SEJIGENT program (REF: **SEJI/2020/007**) and Universitat Jaume I from the project of PLA DE PROMOCIÓ DE LA INVESTIGACIÓ (REF: **UJI-A2019-04**).



**Barcelona
Supercomputing
Center**

Centro Nacional de Supercomputación



RES
RED ESPAÑOLA DE
SUPERCOMPUTACIÓN

Total computational time of **600.8 KHours** granted on Pirineus machine is for period of 4 months 1/11/2020 - 28/02/2021

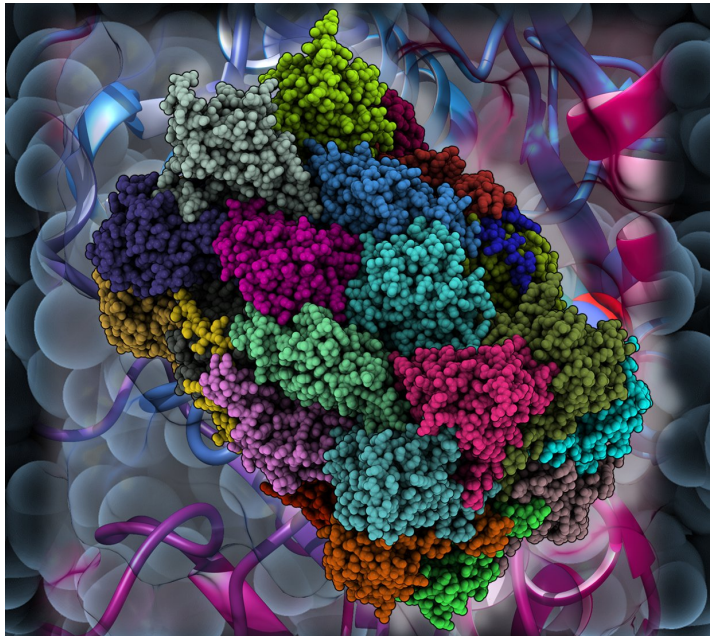
T·R·I·N·I·T·Y cluster: 96 CPUs and 2 NVIDIA RTX 3090 24 GB GDDR6X Blower funded by Ministerio de Ciencia, Innovación y Universidades (REF: **ID2019-107098RJ-I00**)

BioComp group <http://www.biocomp.uji.es/>

StopProt project <http://www.biocomp.uji.es/swiderek/home.html>

QM/MM STUDIES ON THE INHIBITION OF HUMAN 20S PROTEASOME

THE ROLE OF ELECTROSTATIC EFFECTS IN BIOCATALYSIS



UJI UNIVERSITAT
JAUME I

Katarzyna Świderek
Biocomp group, Universitat Jaume I, Spain

BioComp group <http://www.biocomp.uji.es/>

StopProt project <http://www.biocomp.uji.es/swiderek/home.html>

